



Assessing long-term future climate change impacts on extreme low wind events for offshore wind turbines in the UK exclusive economic zone

Sara Abdelaziz^{a,*}, Sarah N. Sparrow^a, Weiqi Hua^b, David C.H. Wallom^a

^a Oxford e-Research Centre, University of Oxford, Oxford, United Kingdom

^b School of Engineering, University of Birmingham, Birmingham, United Kingdom

HIGHLIGHTS

- The research examines different cut-in thresholds of 3 m/s, 4 m/s, 5 m/s, and 6 m/s for low wind speed events.
- Seasonal low wind speed analysis using the 4 m/s threshold shows summer and autumn with the longest durations.
- The seasonal variations in low wind speed event durations under the 4 m/s threshold demonstrate that summer and autumn have the most extended durations of low wind speed.

ARTICLE INFO

Keywords:

Climate change
Low wind speed event
Extreme weather event
Return time

ABSTRACT

The impacts of climate change must be considered while planning offshore wind turbines (OWT), as it will result in more frequent and severe weather extremes. To ensure the dependability and affordability of wind energy, it is necessary to address extreme low wind speed events (LWE). This study aims to assess the reliability of wind power in the future by analyzing the rise of low wind durations and intensities in two future periods, 2021–2040 and 2061–2080, compared to the historical period of 1981–2000. The research compares the results for four main regions in the UK EEZ: East, South, West, and North. We examine different cut-in thresholds of 3 m/s, 4 m/s, 5 m/s, and 6 m/s in the UK exclusive economic zone (EEZ). The seasonal variations in LWE durations <4 m/s demonstrate that summer and autumn have an increase in most of the LWE durations occurrence in the 2061–2080 period in all regions compared to the historical period. Using five days running mean wind speed, the return time for 6 m/s cut-in wind speed shows that OWT will be vulnerable to frequent extreme LWE in most areas, with most sites experiencing a return period of up to 20 years. According to the return year region median and the Risk Ratio (RR) calculations, it is suggested that the South region exhibits a diminished risk of experiencing more frequent instances of wind speeds surpassing the cut-in threshold, specifically when utilizing cut-in thresholds of 5 m/s and 6 m/s, during the period spanning 2021–2040, as compared to the historical period. Furthermore, when employing 6-, 7-, and 8-day running means, the analysis reveals that the return period for wind speeds of 4 m/s in the Western region remains consistently recommended throughout the 2021–2040 period. In contrast, utilizing a 6-day time window for assessing the return period of 4 m/s wind speeds indicates a notable escalation in risk across all regions during the 2061–2080 period.

1. Introduction

Wind energy is one of the key renewable resources we must exploit to meet the 2-degree Paris Agreement target [1]. To meet the energy demand, the first commercial-scale offshore wind turbine (OWT) was established in 2002 in Denmark [2]. Recently, extensive efforts have

been made to expand offshore wind farms (OWF) in deep water [3]. Wind potential is an indicator of the percentage of electricity produced in different regions and, therefore, the economic viability of the investment [4]. The general understanding of wind velocities in the wind turbine (WT) production phase has been studied extensively [5–9]. Also, wind energy production is widely investigated in the context of climate change [7,10,11]. In contrast, less research has investigated the

* Corresponding author.

E-mail addresses: Sara.abdelaziz@eng.ox.ac.uk (S. Abdelaziz), sarah.sparrow@oerc.ox.ac.uk (S.N. Sparrow), w.hua@bham.ac.uk (W. Hua), david.wallom@oerc.ox.ac.uk (D.C.H. Wallom).

<https://doi.org/10.1016/j.apenergy.2023.122218>

Received 4 June 2023; Received in revised form 15 September 2023; Accepted 30 October 2023

Available online 9 November 2023

0306-2619/© 2023 The Authors. Published by Elsevier Ltd. This is an open access article under the CC BY license (<http://creativecommons.org/licenses/by/4.0/>).

Nomenclature

OWF	Offshore wind farms
RCP	Representative Concentration Pathway
RMSE	Root Mean Square Error
EEZ	Exclusive economic zone
ERA5	Fifth generation ECMWF atmospheric reanalysis of the global climate
GEV	Generalized Extreme Value
OWT	Offshore wind turbines
CPM	Convection permitting climate model projections
K-S	Kolmogorov-Smirnov
LWE	Low wind speed event
MSLP	Mean sea level pressure
MSE	Mean absolute Error
IQR	Interquartile ranges
UKCP18	UK Climate Projection 2018
WT	Wind Turbine
CDF	Cumulative distribution function
~	Approximately

persistence of extremely low wind speeds events (LWE) and their variability. However, still weather has noticeably affected wind generation [12]. For instance, Scottish and Southern Electricity, a UK-based power company, said that its renewable assets produced 32% less power than expected in the period from 1 April 2021 to 22 September 2021, and an 11% decrease in forecast total output for the full year [12]. Also, the latest United Nations Intergovernmental Panel on Climate Change (IPCC) report suggests that average wind speeds over the European region will reduce by 8%–10% as a result of future climate change [13–15].

Siting OWFs is a topic that gained more attention from researchers because of the promising features of offshore areas compared to onshore locations. Several models in the literature have been introduced to investigate OWF siting by choosing optimal areas for multivariate activities and facilities [16–22]. These models use multi-criteria decision analysis to estimate the best OWF locations, considering criteria such as wind speed, water depth, distance to shoreline, and the grid to select the most suitable location for siting OWFs. On the other hand, few studies considered coupling the future climate change and extreme weather events occurrence and severity with the future planning of wind energy from a spatial perspective [11,23–27]. Extreme weather events are expected to occur more often due to climate change; they must be accounted for with an in-depth assessment of their duration and severity during the spatial planning of future OWF. Estimating extreme wind speeds is a critical component of WT design for capital costs, structural integrity, and site selection [25]. Investigating the persistence of LWE is centered on two methods. The first uses a certain capacity factor threshold to count consecutive days below that threshold [28–31].

The second method uses one or more cut-in wind speed thresholds to investigate LWE. Here, we focus on literature that tackles the second method for investigating LWE, as this research mainly focuses on utilizing cut-in wind speed threshold to identify extreme LWE. In 2017, Patlakas et al. [32] used 10 years of the MARINA database to investigate LWE in five North Sea locations. The study used a wind speed threshold of 3 m/s to identify low wind durations and found that most events have a 4-to-5-day duration in open sea areas. In Leahy and McKeogh [33], durations of 1 h to 20 days were investigated for LWE in Ireland. The research uses a running mean to match each of the durations selected in the study, and the annual minimum was used following Khaliq et al. [34] approach that calculates heatwave duration and frequencies from daily maximum temperature records. The probability of remaining below thresholds of 4 m/s, 6 m/s, and 10 m/s was investigated, and it was

shown that sustained LWE lasting 20 days have return periods (using a Gumbel distribution) of around ten years for near-shore areas. Using ERA-Interim Reanalysis, Weber et al. [35] calculated the durations of persistent LWE under the 4 m/s threshold. The durations are used to investigate wind persistence statistically. The research found that q -exponential distributions had a good performance fitting the duration data all over Europe.

We have concluded from the existing literature that, although LWEs are rare, they can last for several days and lead to significant issues for the power system as a no power output from WT leads to generation loss. Moreover, using more than one distribution to assess the data best fit is highly recommended, especially for studies considering extreme weather events (which focus on heavy tails). To the extent of the author's knowledge, all persistent LWE investigations are conducted using historical wind speed data, and there is no consideration for future warming periods. However, investigating climate change signals can ensure a reliable and economically feasible future energy system. Analyzing durations and magnitude of LWE are desired to construct a comprehensive understanding of LWE risk in current and future warming periods and optimize locations for future wind resource development.

This research focuses on LWE that occurs below cut-in wind speed values in the UK Exclusive Economic Zone (EEZ). The main key contributions of this work are:

- Quantifying the seasonal change in low wind speed in the mean of the distribution and the future change in the 8th percentile of wind speed for all locations in the UK EEZ.
- Examining the frequency and duration of low wind speeds seasonally in future warming scenario Representative Concentration Pathway (RCP) 8.5.
- Investigating the likelihood of different LWE magnitudes using multiple time windows.

The research is organized as follows: Section 2 provides the necessary information for the climate model used and the chosen WT model. Section 3 illustrates the process of selecting the four regions in the UK EEZ. In Section 4 the four methods of low wind speed analysis are described, including investigating the seasonal variation of daily mean wind speed and 8th percentile of wind speed, analyzing the future changes in low wind speed duration, and illustrating the return periods for LWE magnitudes of 4 m/s, 5 m/s, and 6 m/s using a 5-day running mean and the return periods for a 4 m/s LWE using running means of 7-, 8-, and 8-days. Sections 5 and 6 provide the discussion and the conclusion for the paper findings.

2. UKCP18 climate model

This study utilizes daily mean surface wind speed data obtained from convection-permitting climate model projections (CPM) generated as part of the UKCP18 project [36,37]. The provided data encompasses climate changes for the UK until 2080, downscaled to a horizontal resolution of 2.2 km [38]. The UKCP18 dataset encompasses three distinct periods: the baseline period (1981–2000), representing historical climate conditions, and two future periods, representing the near future (2021–2040) and the far future (2061–2080). Both future periods align with the RCP8.5 scenario, characterized by an estimated global average temperature increase of 4.3 °C by 2100 compared to pre-industrial levels [36]. Currently, the 2.2 km UKCP18 UK grid only provides the RCP8.5 pathway.

The UKCP18 model simulations comprise 12 ensemble members, each representing climate variability within a changing climate context. The UKCP18 CPM is a recently established model that primarily focuses on the analysis of land area [36,39–41]. In this study we verify the entire distribution of daily mean wind speed used in this analysis to understand the future change in the mean of the distribution and in the distribution

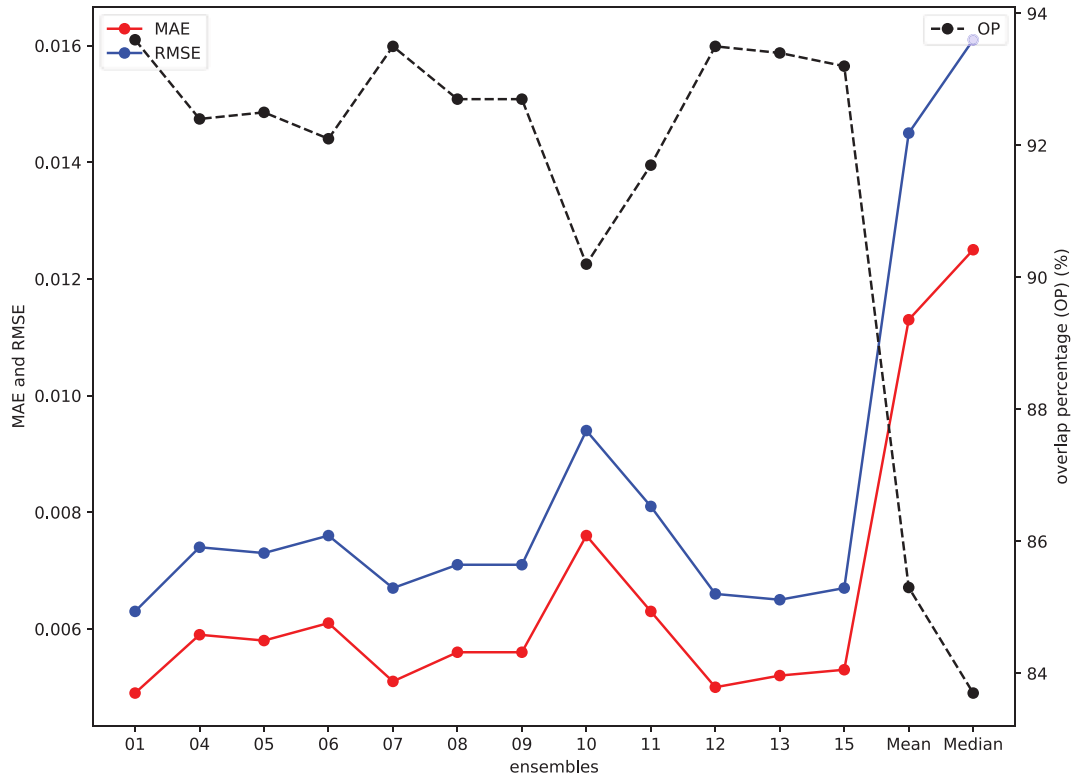


Fig. 1. The OP (%) (black line), MAE (red line), and RMSE (blue line) of mean wind speed are calculated for the 12 ensembles and (a) and (b) refer to the ensembles mean and median for the period 1981–2000, respectively. The values in the plot represent the mean of all EEZ cell grids. (Colour should be used in print). (For interpretation of the references to colour in this figure legend, the reader is referred to the web version of this article.)

left tail (extreme low wind speed), as both are considered essential for assessing the future wind generation.

We seek to compare the 12-ensembles of the UKCP18 model's daily mean wind speed that covers the UK EEZ against the ERA5 (fifth generation ECMWF atmospheric reanalysis of the global climate) reanalysis model [42]. The ERA5 reanalysis combines observations from various sources worldwide with model data to generate a dataset that exhibits global consistency. It has been extensively utilized in wind energy assessment studies [43–45] and serves as a benchmark for validating model projections [11]. We aim to identify the UKCP18 ensemble, or the ensemble mean/median, demonstrating the closest statistical resemblance to the ERA5 reanalysis from 1981 to 2000. The UKCP18 ensembles have been remapped to a spatial resolution of $0.25^\circ \times 0.25^\circ$, similar to the ERA5 resolution, to facilitate a meaningful comparison between the two datasets.

The objective is to evaluate the ability of each ensemble in the local climate model to replicate wind patterns. The overlap percentage (OP) analysis, previously employed for validating offshore wind speed projections [46–49], is adopted in this investigation. The OP analysis is used to spatially compare the extent of overlap between the probability density function (PDF) derived from the ERA5 dataset and that obtained from the UKCP18 dataset within the UK EEZ, focusing on the historical period spanning from 1981 to 2000. The OP calculation is as follows:

$$OP = \sum_{i=1}^n \text{minimum}(h_m, h_0) * 100 \quad (1)$$

Where OP is the overlap percentage, n is equal to 26 and represents the number of bins used to calculate pdf; h_m and h_0 are the UKCP18 and ERA5 frequency values, respectively. When the OP is equal to 100%, it indicates that the corresponding UKCP18 ensemble has effectively replicated the local wind speed projections.

Fig. 1 summarizes the OP, mean absolute error (MAE), and root mean absolute error (RMSE) results, considering the average values across the

entire EEZ. The OP represents the degree of overlap and exhibits an average value of 92.6% across the 12 ensembles. The ensemble's mean and median are 85.3% and 83.7%, respectively. The average MAE for the 12 ensembles is 0.0057, while 0.0113 and 0.0125 are the MAE for the ensemble mean and median, respectively. The average RMSE is 0.0072, and 0.0145 and 0.0161 are the RMSE ensemble mean and median, respectively. The analysis reveals that the ensemble mean and median display less desirable values for OP, MAE, and RMSE. Conversely, for the baseline period of 1981–2000, we identified the highest level of agreement with the ERA5 reanalysis model within ensembles 01, 07, and 12 over the UK EEZ. Given the significant computational challenge this research use ensemble 01, conducting the analysis utilizing other ensembles was not feasible due to the considerable time required for processing. It is recommended to reproduce the analysis utilizing the remaining eleven ensembles and use the sensitivity analysis techniques to determine the impact of the varying ensembles on the results. Such an approach would substantially reduce the uncertainty arising from climate models.

Multiple WT models with different capacities are used in the literature, each affects wind energy production in UK offshore areas. In this research, we investigate the future change in wind speed; consequently, using a WT model estimated to be installed in the future is preferred. By 2035, it is anticipated that the capacity of future WTs will reach 17 MW, accompanied by a hub height of 151 m [50]. We adopted this turbine model in this research. Building upon that foundation, we scaled the wind speed to a WT hub height of 151 m using an empirical relationship [51,52].

3. Adopted UK offshore regions

The EEZ was established in 1982 during the third United Nations Conference on the Law of the Sea. It delineates a maritime area wherein a sovereign state possesses special rights pertaining to various resources,

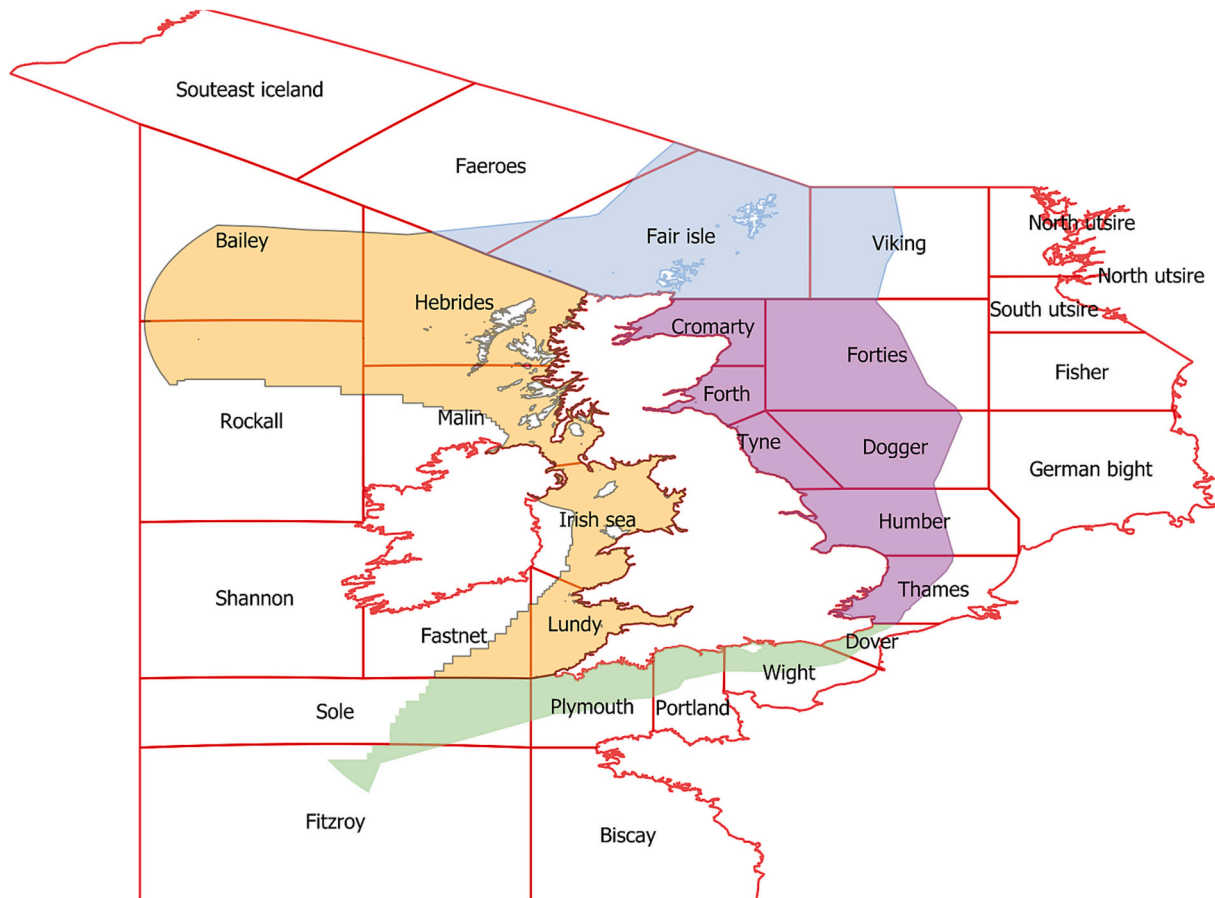


Fig. 2. The outer boundary is the UK EEZ. The inner boundary (between the green (South), yellow (West), blue (North), and purple (East) regions) are the boundaries for the four considered region within the EEZ for investigating best region for future OWF installation. (For interpretation of the references to colour in this figure legend, the reader is referred to the web version of this article.)

Table 1

The merged shipping areas for the East, South, West, and North regions.

Region	East	South	West	North
Included coastal sea areas	Cromarty, Forth, Forties, Tyne, Dogger, Humber, Thames,	Portland, Wight, Dover, Malin, Sole, Plymouth	Hebrides, Irish sea, Lundy, Fastnet, Bailey, Rockall,	Viking, Faeroes, Fair Isle

such as wind and water energy production. The EEZ extends up to 200 nautical miles from the coastal baseline [53]. Traditionally, marine weather forecasts in the UK have been formulated as shipping forecasts, with distinct weather areas corresponding to each shipping region. Beginning in 2002, the UK offshore territories were divided into 31 shipping forecast areas [54]. In line with these defined areas, this study employs the boundaries of the shipping forecast regions to define four primary homogeneous wind regions within the UK EEZ, namely East, South, West, and North (see Fig. 2). Each of these regions is enclosed within the EEZ mask. The only available data from UKCP18, which intersects with the EEZ, has been considered for analysis, see Table 1. This paper primarily focuses on comparing the findings across the four defined regions. However, it is essential to mention that UKCP18 (2.2 km) is solely available within a latitudinal range up to 60.58° N, thus excluding the northernmost region of the EEZ (latitude boundary at 63.5° N). Consequently, the results presented in this study are limited to the truncated region below 60.58° N.

4. Future change in low wind speed

We build our understanding of the future change of low wind speed on four principal analyses used to investigate different meteorological aspects of wind speed. The next four sub-sections illustrate these aspects. The first aspect is the future change in the entire distribution of the mean wind speed, where the change in the mean of the distribution can be detected, corresponding to the range of wind speed associated with energy production. The second aspect is to investigate the instantaneous change in wind speed in the future under a certain percentile, which shows us the amount of change in the left tail of the distribution in the two future periods compared to historical periods. The third aspect is focused on investigating the duration of low wind speed under multiple cut-in wind speed thresholds. The fourth aspect investigates the probability of future reoccurrences of multiple low wind speed event definitions using different time windows and wind speed thresholds.

4.1. Change in daily mean wind speed distribution

To investigate the impact of the warming scenario on future wind production, we use the cumulative distribution function (CDF) to analyze future changes in wind speed distribution. Fig. 3 presents the future wind speed distribution in the UK EEZ through the CDF and future wind speed distribution in four regions of the UK. All analysis is based on the daily mean wind speed dataset. In Fig. 3, the summer and autumn seasons in all regions exhibit a shift toward lower wind speeds in one or two of the future periods compared to the baseline period, indicating the presence of lower wind speeds in these seasons. This supports the findings in [29,55], where a substantial increase in low wind episodes

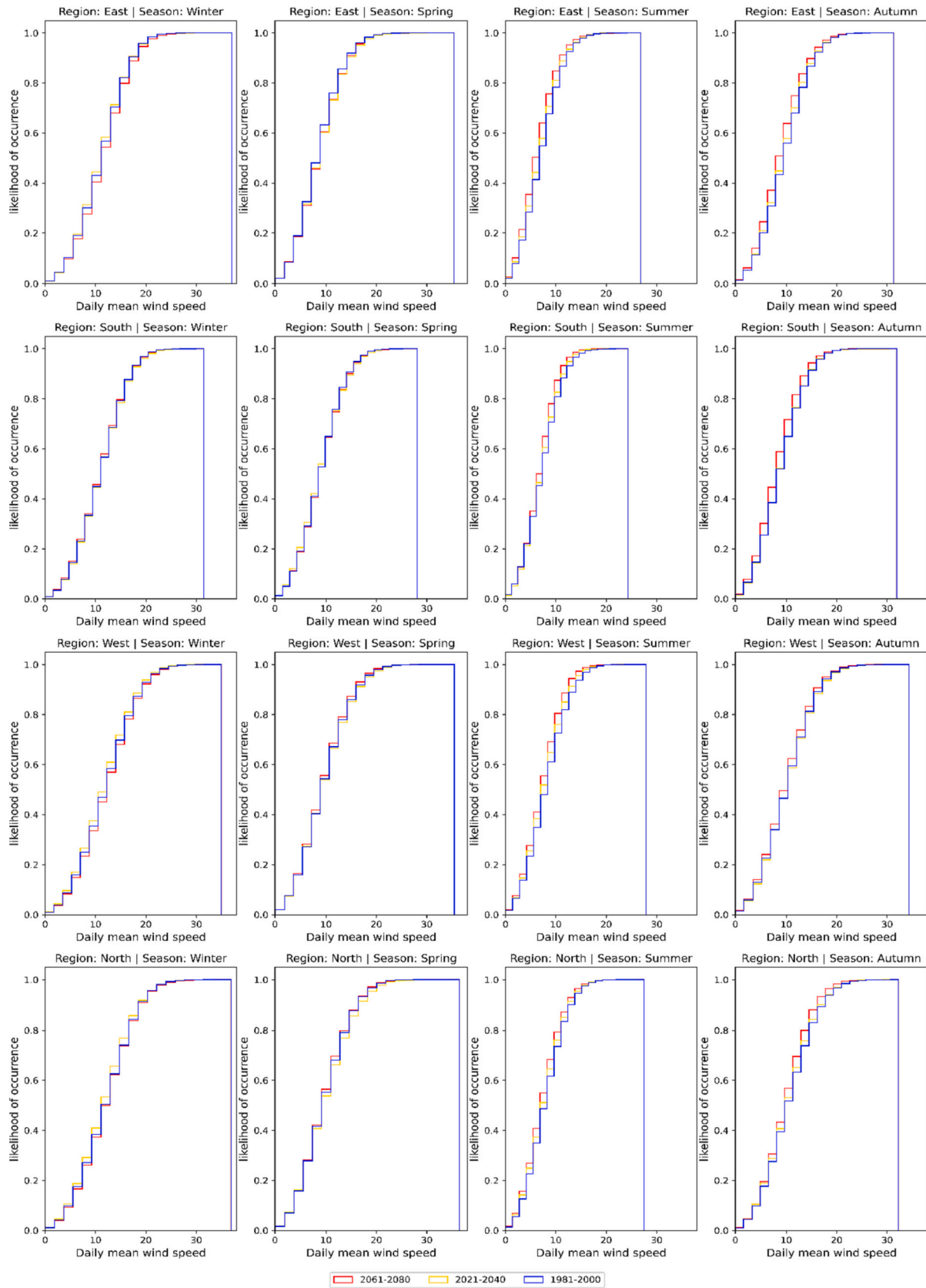


Fig. 3. Cumulative distribution function plots of daily mean wind speed. Blue, yellow, and red represent the 1981–2000, 2021–2040, and 2061–2080 periods, respectively. Rows represent the four regions: East, South, West, and North. Columns represent the four seasons from left to right: winter, spring, summer, and autumn. Blue, yellow, and red indicate the 1981–2000, 2021–2040, and 2061–2080 periods. (Colour should be used in print). (For interpretation of the references to colour in this figure legend, the reader is referred to the web version of this article.)

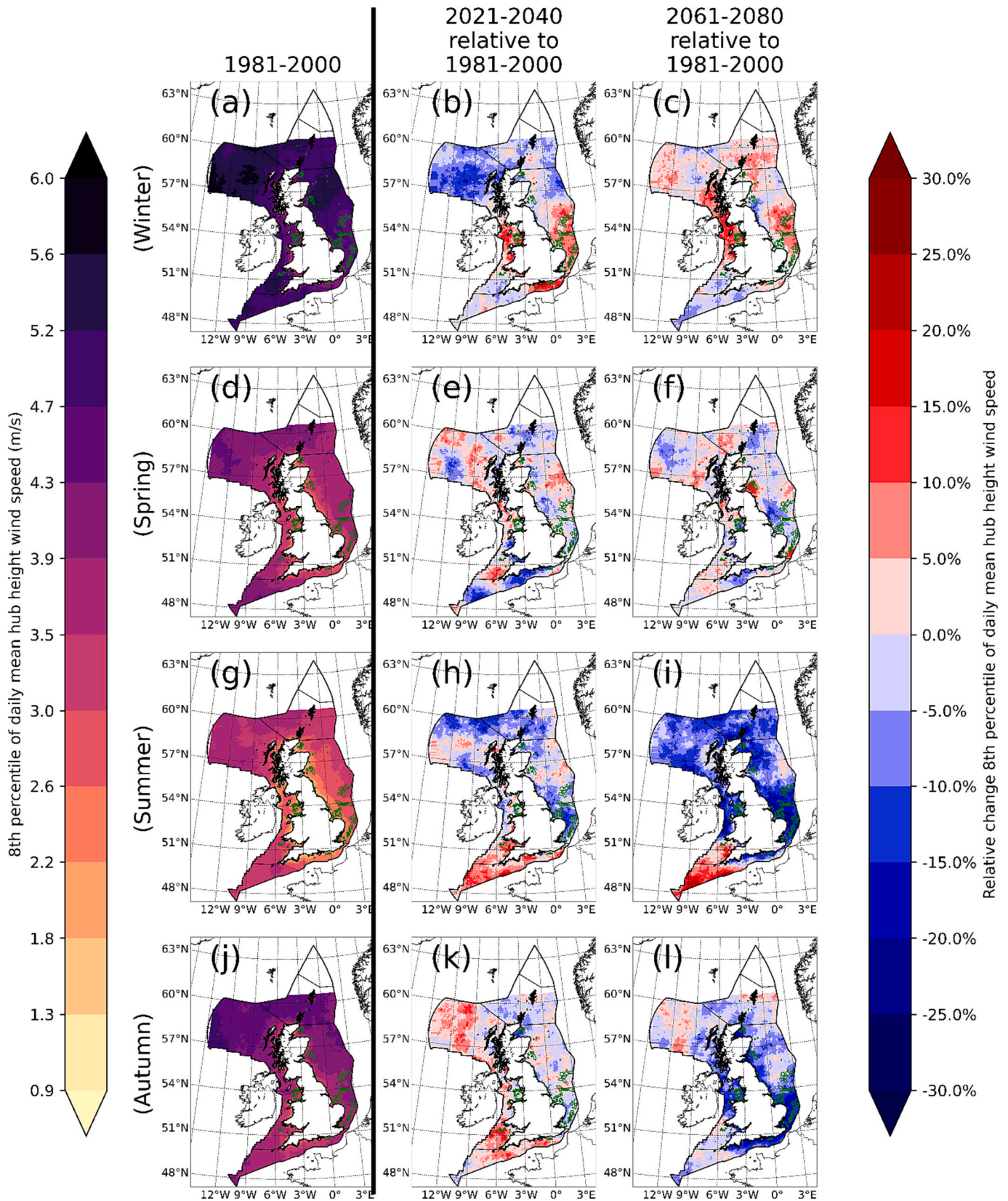


Fig. 4. Column 1 from left side: 8th percentile of daily mean hub height wind speed in the four seasons for the 1981–2000 period. Rows from 1 to 4 represent the four seasons: winter, spring, summer, and autumn. Column 2 and 3 from the left side: shows the relative change of 2021–2040 and 2061–2080 to 1981–2000, respectively. The green lines represent the UK Contract for bidding rounds: Round 1, Round 2, Round 3, and Round 4, and the floating wind farms location, see supplementary material for wind farms names. (Colour should be used in print). (For interpretation of the references to colour in this figure legend, the reader is referred to the web version of this article.)

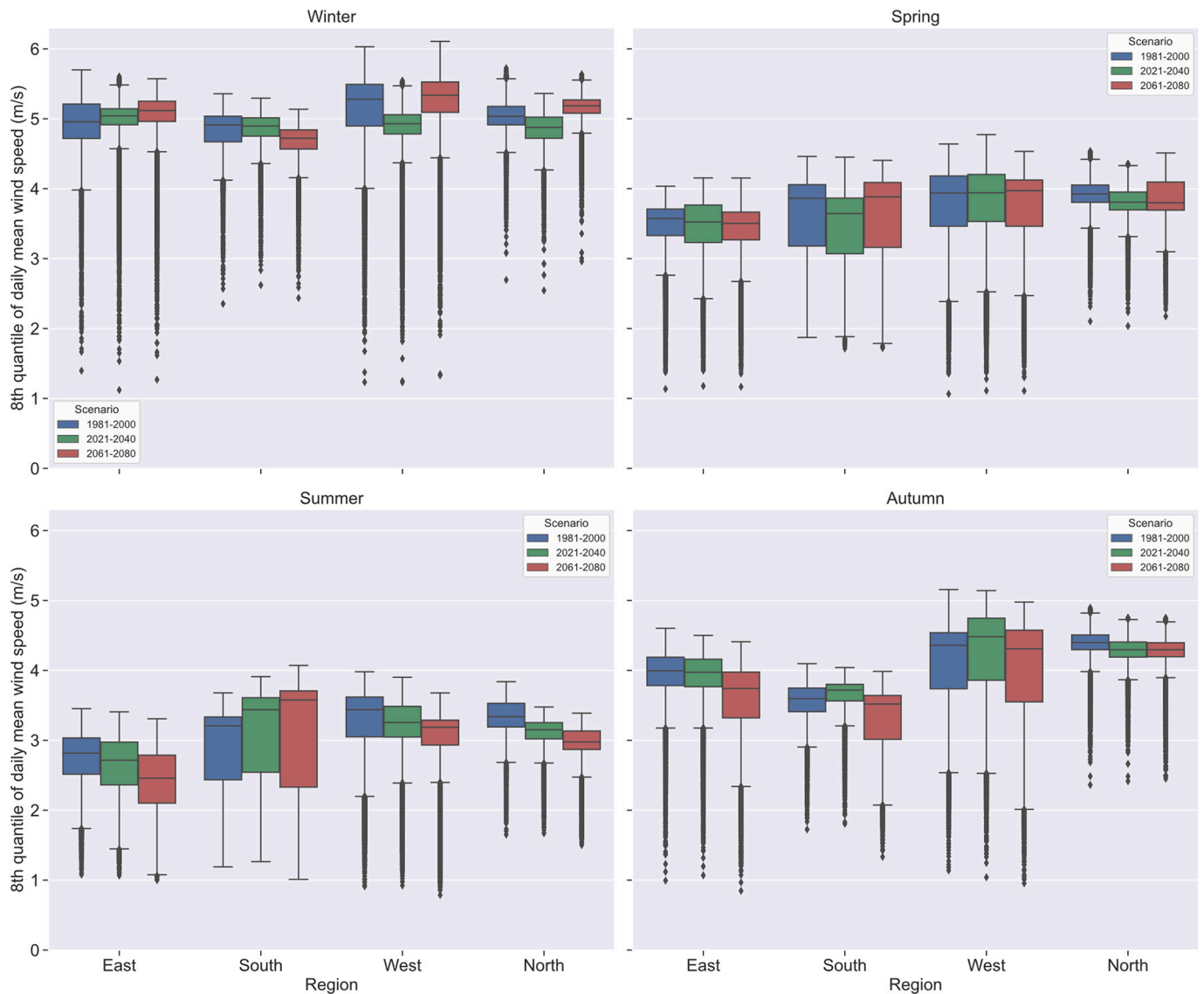


Fig. 5. Box plot to compare the 8th percentile of daily mean wind speed for three periods (1981–2000 (blue), 2021–2040 (green), 2061–2080 (red)) among four seasons (winter, spring, summer, and autumn). In each plot, the four panels of comparison are the four regions, East, South, West, and North. The box holds the interquartile ranges (IQR), and the midline represents the median. The whiskers show the maximum and minimum values. The thin vertical black line represents the rest of the distribution, except for points determined to be “outliers”. (Colour should be used in print). (For interpretation of the references to colour in this figure legend, the reader is referred to the web version of this article.)

was observed in the summer compared to the winter. On the other hand, in the summer season, for wind speed < 5 m/s in the South region, there is no change in the 2061–2080 periods compared to the historical period and a slight decrease of low wind in 2021–2040 compared to the historical period.

Moreover, in the autumn season, there is no increase in wind speed for the 2021–2040 period compared to the historical period in the South and West regions. In the winter season, the West and North regions witness a notable decrease in wind speed compared to the historical period in the near future (2021–2040). In the spring season, the empirical CDF for these two regions shows a slight decrease in wind speed in the far future (2061–2080) compared to the historical period (1981–2000).

4.2. 8th percentile daily mean wind speed

Energy generation by WTs requires wind speeds within a specific range, defined by the cut-in value (minimum wind speed) and cut-off

value (maximum wind speed) [56]. When wind speeds are too low, the torque generated by the air is insufficient to rotate the WT blades, resulting in the inability to produce energy. The wind speed at which the WT blades start to spin and convert mechanical energy into electrical energy is known as the cut-in wind speed, typically ranging from 3 m/s to 6 m/s [32–35,57]. This section examines the future changes in low wind speeds at the 5th, 6th, 7th, 8th, and 10th percentile to determine at which percentile we have a range of wind speed across all seasons that covers the most common values of cut-in wind speed (< 6 m/s). By defining the percentile that best matches the most common range of cut-in wind speed thresholds across the four seasons, we will be able to estimate the change in the two future periods by applying the percentile value on the three climate periods and quantify the change in the corresponding wind speed for the two future periods compared to the historical period.

We found that the 8th percentile best represents the cut-in wind speed of < 6 m/s across all seasons, which will be discussed in this section. The future changes in the 5th, 6th, 7th, and 10th percentile can be

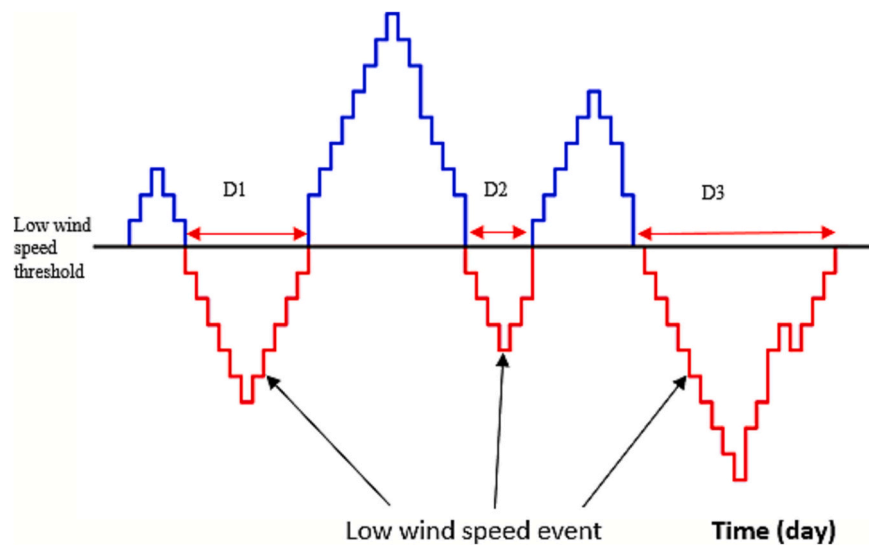


Fig. 6. The schematic diagram for LWE durations. The black horizontal line is the cut-in wind speed thresholds used in this research (3 m/s, 4 m/s, 5 m/s, and 6 m/s). The red line represents the periods of LWE, and the blue line represents the periods above thresholds, so they are not calculated for LWE. D1, D2, and D3 are the durations calculated from the number of days that occurred under a certain threshold. (Colour should be used in print). (For interpretation of the references to colour in this figure legend, the reader is referred to the web version of this article.)

found in the supplementary material. Maps showing the 8th percentile for each season are depicted in Fig. 4 (a), (d), (g), and (j) using the 1981–2000 period. During the winter, the highest range of low wind speed is observed, averaging between approximately (\sim) 4 to 6 m/s.

Conversely, the lowest values for the 8th percentile are recorded in the summer, ranging from 1 to 4 m/s. The 8th percentile wind speed is lowest near coastline areas compared to open sea areas across the four seasons. In columns 2 and 3, the relative change for the two future

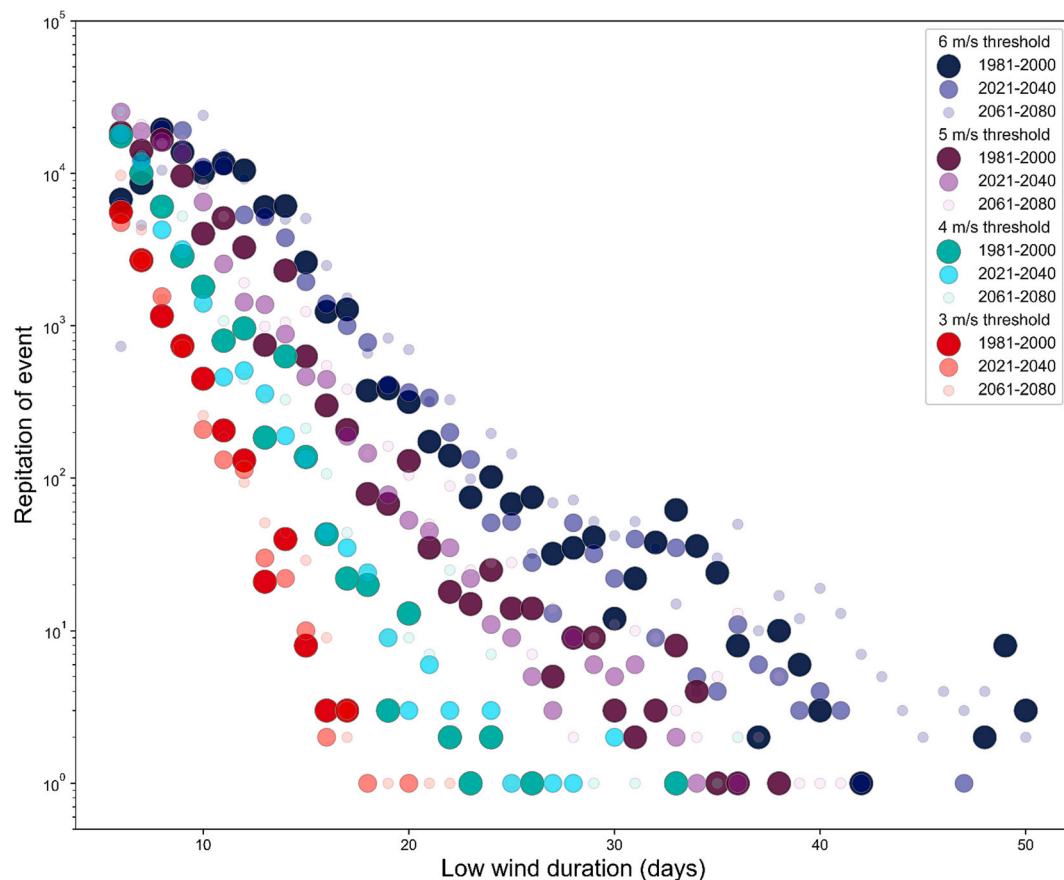


Fig. 7. Scatter diagram for low wind speed durations. Blue, purple, green, and red shades represent durations under 6 m/s, 5 m/s, 4 m/s, and 3 m/s. The changing size of the circle between periods is used to show the overlap data and does not indicate any additional weighting for periods. The x-axis represents the maximum spatial durations of low wind speed; only durations greater than and equal to five consecutive days are shown. Y-axes represent the corresponding repetition for each duration. (Colour should be used in print). (For interpretation of the references to colour in this figure legend, the reader is referred to the web version of this article.)

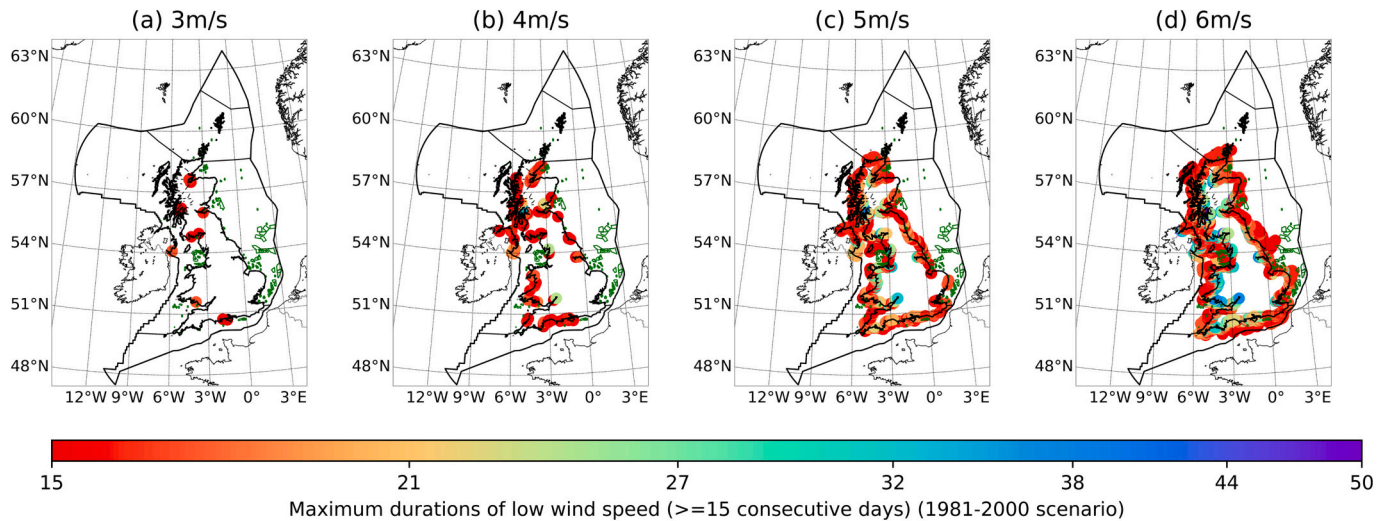


Fig. 8. Greater than or equal to 15 consecutive days of low wind durations in the 1981–2020 period. The count of consecutive days has been done for three thresholds: (a) 3 m/s, (b) 4 m/s, (c) 5 m/s, and (d) 6 m/s. (Colour should be used in print).

periods is calculated as follows:

$$RC = (V_j - V_i) / (V_i) \quad (2)$$

The relative change (RC) of wind speed is calculated as the difference between the wind speed in the future (V_j) and the historical wind speed (V_i). A negative relative change percentage (blue shades in Fig. 4, column 2 and 3) indicates a shift toward a smaller wind speed value in the left tail of the wind speed distribution in the location, indicating a prone location for extremely low wind speed in the future. In Fig. 4, the summer season experienced the largest decrease in the 8th percentile with a range of approximately 5% to 25% in the 2021–2040 period compared to the 1981–2000 period in most locations of East, West, and North regions. Meanwhile, the north-west of the UK experiences a decrease in wind speed in the winter season. The 2061–2080 period also shows a reduction in wind speed in most regions during the summer, except for the South.

Fig. 5 shows the statistical representation of Fig. 4, where the region median, the 25 quantiles, and 75 quantiles are calculated for each region in the four seasons. Fig. 5 shows that the median low wind speed in the future is decreasing in the East, West, and North regions during the summer, while the South region has the lowest risk of reducing wind speed. The autumn season in the 2061–2080 period has a lower median of 3.6 m/s compared to 4 m/s in the baseline period for the East region. During the winter season, the 2021–2040 period shows a decreasing median in the West and North regions compared to the baseline period. In conclusion, the wide distribution of low wind speeds reveals ample opportunities to plan major OWF maintenance during the summer months in the two potential future periods. On the other hand, alternative energy generation and storage solutions must also be considered to overcome the lack of wind energy during this time.

4.3. Duration of low wind speed events under 3 m/s, 4 m/s, 5 m/s, and 6 m/s thresholds

The production of low renewable energy for an extended period, such as several days, can put pressure on the electricity system, particularly during high demand periods [58]. The persistence of LWE can be determined similarly to the calculation of drought events, both of which are measured by counting the consecutive hours, days, or months that fall below a certain threshold [35,59,60]. The standardized precipitation index (SPI) is widely used as a threshold in drought analysis, but it is also important to note that various indices have been utilized [60]. In this study, we have established thresholds specific to the wind energy

industry and represent a safe level of WT power generation. Fig. 6 shows how the LWE is calculated by counting the entire period (in red) when the daily average wind speed drops below the cut-in wind speed threshold (black horizontal line) until it rises above the threshold again. The consecutive days under this threshold are recorded as LWE for historical data and two future periods. Fig. 7 shows the repetition of LWE for durations >5 days, with cut-in speeds of 3 m/s, 4 m/s, 5 m/s, and 6 m/s, computed spatially from historical data and two potential future periods. The durations that surpass five continuous days are taken into consideration, as they are considered the starting point of potential stress on electricity generation [28]. A noticeable variation is evident between the durations under different speed limits, with the most notable occurrence of low wind speed durations happening at the higher cut-in wind speed thresholds. Additionally, as expected, the repetition of durations under higher cut-in thresholds is more pronounced than lower ones. A common pattern among all durations under all thresholds is the high repetition frequency for events with short durations, as opposed to others with longer durations. It is also worth noting that the baseline and future periods under any threshold have higher repetition values than those under lower thresholds. The maximum number of consecutive days observed under 3 m/s, 4 m/s, 5 m/s, and 6 m/s are approximately 20, 30, 40, and 50 days, respectively. As seen, there is a difference of ten consecutive days between the maximum durations recorded for the four cut-in thresholds.

Durations lasting 15 or more consecutive days are found near the UK coastline. Fig. 8 presents LWE lasting 15 or more consecutive days for the 3 m/s, 4 m/s, 5 m/s, and 6 m/s thresholds using the 1981–2000 period. The longest durations under each threshold are all situated close to the UK coastline, which confirms findings from Patlakas et al. [32] that there were 20 consecutive days of low wind speed over ten years near the UK coastline in the North Sea. As stated by Patlakas et al. [32], the main reason for these extremely high durations near-shore areas could be the interaction of complex terrain with the atmosphere and its representation within the climate model configuration. Additionally, the flow in areas with complex altitudes, such as coastlines, is challenging due to dynamic and thermodynamic effects, such as channeling, sea-land barriers, and boundary layers. Following Patlakas et al. [32] suggestion that extremely long durations occurring on coastline locations could be a result of the model configuration, we will remove durations greater than or equal to 15 m/s in the investigation of the seasonal variation in low wind speed duration in Fig. 9.

The variability in the prolonged periods of low wind speed across seasons in two future periods compared to the baseline period is

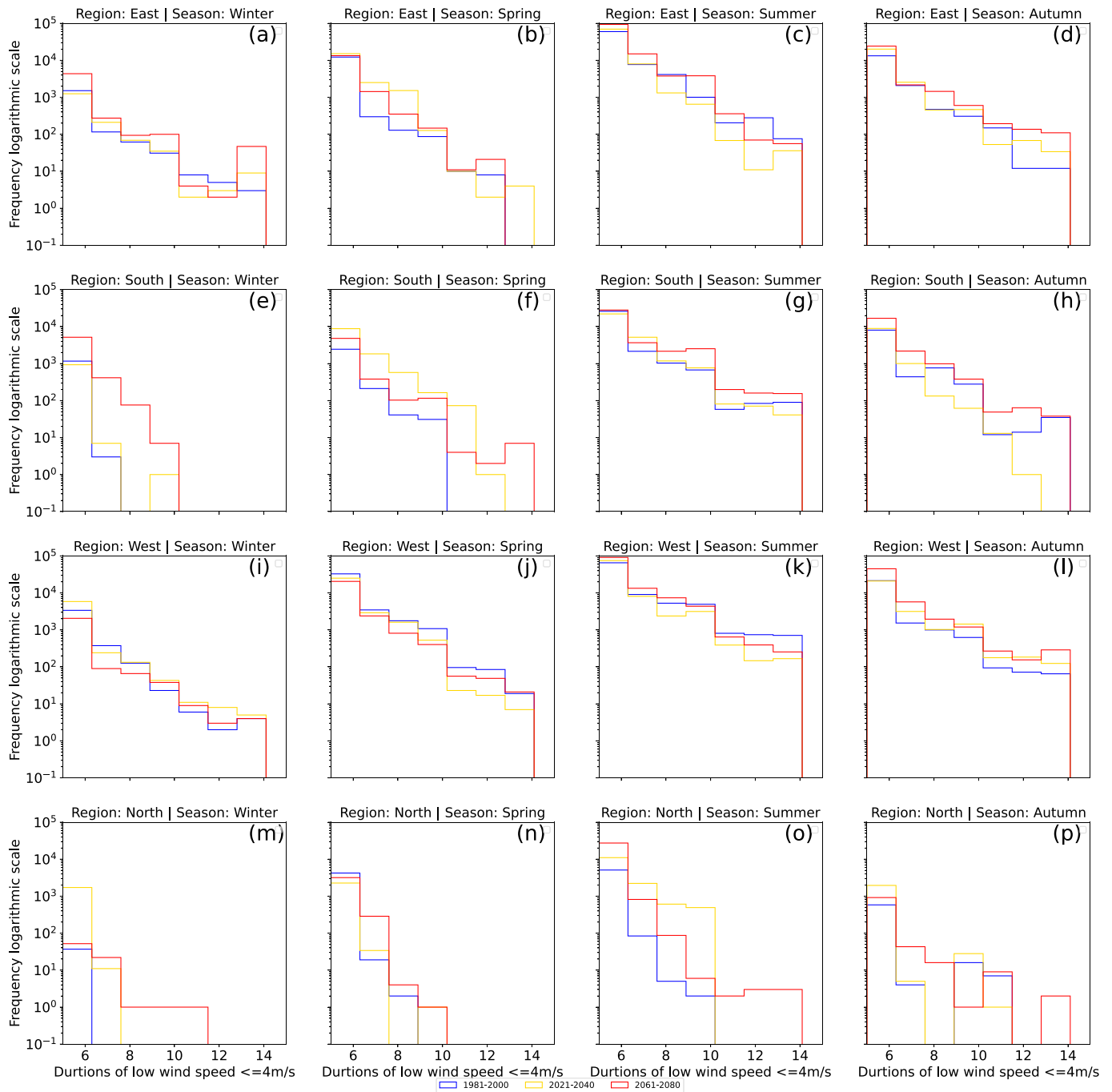


Fig. 9. Histogram of low wind speed durations ≤ 4 m/s. Blue, yellow, and red represent the 1981–2000, 2021–2040, and 2061–2080 periods, respectively. The four rows represent the regions: East, South, West, and North (from top to bottom). Four columns (from left to right) represent the winter, spring, summer, and autumn seasons. (Colour should be used in print). (For interpretation of the references to colour in this figure legend, the reader is referred to the web version of this article.)

analyzed in Fig. 9. The histogram depicts durations lasting between five consecutive days and 15 consecutive days in each cell grid for a 4 m/s threshold, and it is a representation of the maximum duration calculated in each cell grid in the EEZ, where we found that durations lasting <15 days are more concentrated near the coastline and decrease gradually toward the open sea locations. A logarithmic scale represents the frequency of events because of the high frequency of low durations (especially five consecutive days) and the low frequency of high durations (rare LWE). The North region has the smallest range of durations in the spring season, around 5 to 10 days, while the West region has the highest range throughout all seasons for the three time periods, from 5 to 15 days. In most regions and seasons, one or two of the future periods

have more occurrences of longer duration of LWE compared to the baseline period. For example, the South region has increased LWE durations in one or two future periods in all seasons. On the other hand, in the West region, the occurrence of low wind speed duration in the two future periods has a marginal increase compared to the historical period in the spring. In general, the maximum duration values are greater in the summer and autumn seasons in all four regions than in the winter and spring seasons.

4.4. Return year for low wind speed event magnitude pre-processing

The return frequency of LWE can be calculated using the same

Table 2

K-S test, MAE, and RMSE were applied to test fitting GEV, exponential Weibull, and beta distribution to 5-, 6-, 7-, and 8-day running mean using the 1981–2000 period. The percentage of cell grids with P value >0.01 is used to determine the best fitting distribution. The mean and standard deviation of the calculated MAE and RMSE in all cell grids in the UK EEZ is used to determine the best fitting distribution.

Data	Distribution fitting tests 1891–2000 period	Generalized extreme value	Exponentiated Weibull	Beta
5 days running mean	P-value	78.4%	85%	99.9%
	MAE	0.006 ± 0.0009	0.006 ± 0.002	± 0.0007
	RMSE	0.009 ± 0.001	0.009 ± 0.003	± 0.0009
6 days running mean	P-value	72.3%	74.9%	99.9%
	MAE	0.007 ± 0.0009	0.007 ± 0.002	± 0.0007
	RMSE	0.01 ± 0.001	0.01 ± 0.003	± 0.0009
7 days running mean	P-value	70.5%	67.5%	99.5%
	MAE	0.007 ± 0.001	0.007 ± 0.002	± 0.0008
	RMSE	0.01 ± 0.001	0.011 ± 0.002	± 0.001
8 days running mean	P-value	68.1%	61.7%	96%
	MAE	0.008 ± 0.001	0.008 ± 0.002	± 0.0008
	RMSE	0.01 ± 0.002	0.011 ± 0.003	± 0.001

method as for droughts [61]. The probability of recurrence below the cut-in threshold is used to determine the corresponding return year. In 1981–2000, three distributions were used to predict the best fit for the 5-, 6-, 7-, and 8-day running mean data statistics at a hub height of 151 m for each grid cell in the UK EEZ.

These distributions include Generalized Extreme Value (GEV) [62], Exponential Weibull [63], and Beta [64]. MAE, RMSE, and Kolmogorov-Smirnov (K-S) tests were used to evaluate the best-fit distribution for the data [65]. The K-S test uses the P-value to determine the statistical significance of the observed difference, and the alpha value 0.01 represents a 99% confidence level. Table 2 presents the results of the P-values, MAE, and RMSE for the 5-, 6-, 7-, and 8-day running mean data. The results show that the Beta distribution produces the highest percentage of cell grid with a P-value >0.01, equal to 99.9% for the 5 and 6-day running mean data and 99.5% and 96% for the 7 and 8-day running mean data, respectively. Additionally, the Beta distribution has the lowest values for MAE and RMSE.

To demonstrate the method used to determine the return periods or recurrence intervals of LWE, we will use the five-day running mean as an example. Firstly, the running mean of daily wind speed data was calculated for five consecutive days across the spatial domain. The beta distribution of the running mean was then used to calculate the return year for wind speed events that meet the cut-in threshold. This was accomplished through the following equation, which calculates the return period T for events with a magnitude equal to or less than x.

$$T = \frac{1}{F(x)} \quad (3)$$

T is the return time, F(x) is the CDF of beta distribution.

The return time calculation has been done on the historical and the two future periods. In Fig. 10, a single-cell grid shows the return period curve for five days running mean. The black horizontal arrow shows the

wind speed magnitude on the y-axis, and the corresponding vertical arrow indicates the return year on the x-axis.

4.4.1. Return period for 4 m/s, 5 m/s, and 6 m/s using five days running mean definition

Using 5 days running mean wind speed as a representation of possible stress on the electricity grid from low wind generation, we have investigated in this section the probability of returning multiple cut-in wind speed thresholds in future periods. Consequently, we aim to understand the future risk for this event to reoccur and advise about future OWFs situations.

Fig. 11 shows the return years of LWE with 5-day running mean wind speeds <4 m/s, 5 m/s, and 6 m/s. To understand the potential risk of more frequent return time, this study removes return time to >50 years as it does not reflect a high risk. The return time of LWE is larger further from shore than in coastal regions, as more low wind speed datasets occur in the 20 years of data in locations near the coastline compared to open sea due to lower frictional drag across the open sea water's surface compared to near coastline surface. In the three periods shown in Fig. 11 (a) 1981–2000, (b) 2021–2040, and (c) 2061–2080, the return year for 4 m/s <50 years has the smallest spatial coverage compared to the other two thresholds, as it is less likely to have 4 m/s in 5 days window compared to higher value wind speed thresholds. In the 2061–2080 period, the dispersion of return years covers most of the east coast OWF locations, while under higher thresholds such as 5 m/s and 6 m/s, there are even more locations with return years less than or equal to 50 years. Fig. 11(g), (h), and (i) show the return year for 6 m/s extends over the entire EEZ, indicating a higher frequency of LWE events under 6 m/s compared to the other thresholds. The maximum return year values for 4 m/s and 5 m/s are 50 years, while for 6 m/s they are 38 years. To understand the change in the median for the spatial calculation of the return time shown in Fig. 11, we compared the regional median for each of the four regions for the three climate periods in Fig. 12. Fig. 12 shows a trend of decreasing median return years in the two future periods compared to the baseline period for 4 m/s, 5 m/s, and 6 m/s. This suggests a higher risk of more frequent LWE events in the future, except for a slight increase in the median in the North region under 4 m/s and an increasing median in the West region under 5 m/s in the 2021–2040 period.

In addition, the risk ratio (RR) is used to determine the ratio between the likelihood of the event occurring in 2021–2040 (RR 1) and 2061–2080 (RR 2) compared to the occurrence likelihood in the historical climate. The RR approach has been used to define extreme weather events and add confidence to the observed risk in a region [66,67]. The RR is calculated as follows:

$$RR = (F_i/F)/(H_i/H) \quad (4)$$

Where RR is the risk ratio. H_i and F_i are the numbers of data less than the cut-in wind speed threshold in the historical and future periods, respectively. H and F are the total numbers of data available in the historical and future periods, respectively. $RR = 1$ means that the number of values less than a threshold does not affect the specific future period. $RR < 1$ means that the number of values less than a threshold has become less common in the future period. $RR > 1$ means that the number of values less than a threshold increases in the future. In Fig. 13, for the four regions, the RR values under 4 m/s, 5 m/s, and 6 m/s thresholds show a further increase in 2061–2080, similar to the increase from 2021 to 2040, indicating a linear scaling of LWE risk with rising temperatures. In the West region, the median RR value for the 4 m/s threshold in the 2021–2040 period is 1. In the same period, the South region has a median RR value of 1 under 5 m/s and 6 m/s, indicating a lower risk of LWE events below the given thresholds in this climate period. On the other hand, there is a significant increase in risk in the East and North regions in the 2061–2080 period, with the RR of most cell grids above 1. The consistency between the results of return year calculation and the assessment of future RR adds confidence to the

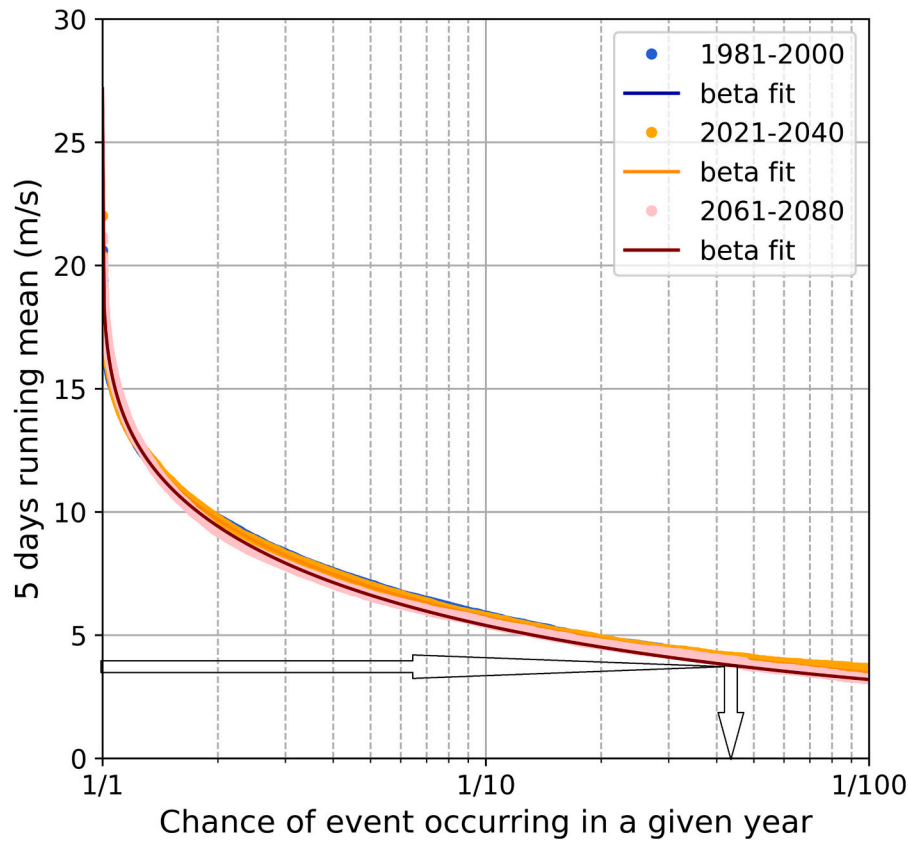


Fig. 10. Return time calculation for 5 days running mean wind speed using beta distribution in a single cell grid for the 1981–2000 (blue), 2021–2040 (yellow), and 2061–2080 (red) periods. The bold black arrows refer to the 4 m/s threshold (y-axis) and the corresponding return year (x-axis). (Colour should be used in print). (For interpretation of the references to colour in this figure legend, the reader is referred to the web version of this article.)

increased risk results in all four regions.

4.4.2. Return period for 4 m/s using 6-, 7-, and 8-days running mean

Investigating the return year in a longer time window for the 4 m/s cut-in wind speed, considered the most common threshold in the literature [19], is crucial to estimating the future risk of LWE and understanding the likelihood of multiple LWE definitions to reoccur in the future. To this end, durations of 6-, 7-, and 8 consecutive days were defined as a set of time windows of interest. The running mean of the daily wind speed time series was calculated for each window, and the extreme value statistics were then applied to determine the return periods. Beta distributions were fitted for the four durations, as mentioned in Table 2. The return year for the 4 m/s threshold was calculated using the 6-, 7-, and 8-day running mean in Fig. 14. As expected, it is less likely to cross the 4 m/s threshold for larger time windows and, additionally, in open sea areas. From (a), (b), and (c) and Fig. 14, across all time windows for the 4 m/s threshold, the likelihood of LWE of this magnitude increases in open sea areas in the future. Fig. 15 shows regional summaries of the spatial results of Fig. 14 in a statistical format. In Fig. 15 (a), for all regions, the six-day running mean shows that the 2061–2080 period has a notable decrease in median compared to the historical period, indicating an increased risk of more frequent low wind energy in all regions. The 2021–2040 period also shows a more marginal median change than the historical period. In Fig. 15 (b) and (c) for 7 and 8 days, respectively, the 2021–2040 period shows a minor change in median compared to the historical period, except for the North region using the eight-day running mean, which indicates an increasing LWE risk in the two future periods compared to the historical period. The 2061–2080 period shows a decrease in median in the South and North regions for the seven-day running mean and, in the South, West, and

North regions for the eight-day running mean.

In Fig. 16, the RR of exceeding the 4 m/s wind speed threshold is calculated for three running mean time windows: 6-, 7-, and 8-days. As seen in Fig. 16 (a), (b), and (c), the 2061–2080 period exhibits higher median RR compared to the 2021–2040 period, signalling an increased risk of reaching the 4 m/s threshold in the latter period. The West region in Fig. 17 (a), (b), and (c) consistently has the lowest risk for both the 2021–2040 and 2061–2080 period. In the 2021–2040 period, the West region's median RR remains at one across all time windows, showing no change in risk compared to the historical period, and in 2061–2080 has a median RR of approximately 1.3.

5. Discussion

We aimed to understand the future change in low wind speed using four different analyses: collectively, the analysis aims to investigate the future change in mean wind speed and extreme low wind speed in the future. Examining the 5th, 6th, 7th, 8th, and 10th percentiles of daily mean wind speed aims to ascertain that the 8th percentile encompasses a range of wind speeds throughout all seasons, including the most prevalent cut-in wind speed values (< 6 m/s). The findings show that the summer season has the lowest wind speeds, as evidenced by the CDF and 8th percentile, reaching between 5% and 25% in all regions except the South of daily mean wind speed. Additionally, the summer season has the longest durations of low wind speed (< 4 m/s). Moreover, it is noted that the two future periods in the autumn season also drop in the majority of the low wind speed durations compared to the historical period, potentially representing an extension of the summer season LWE in the future, except for 2061–2080 period the durations show a decrease compared to the historical period in the South region. These findings

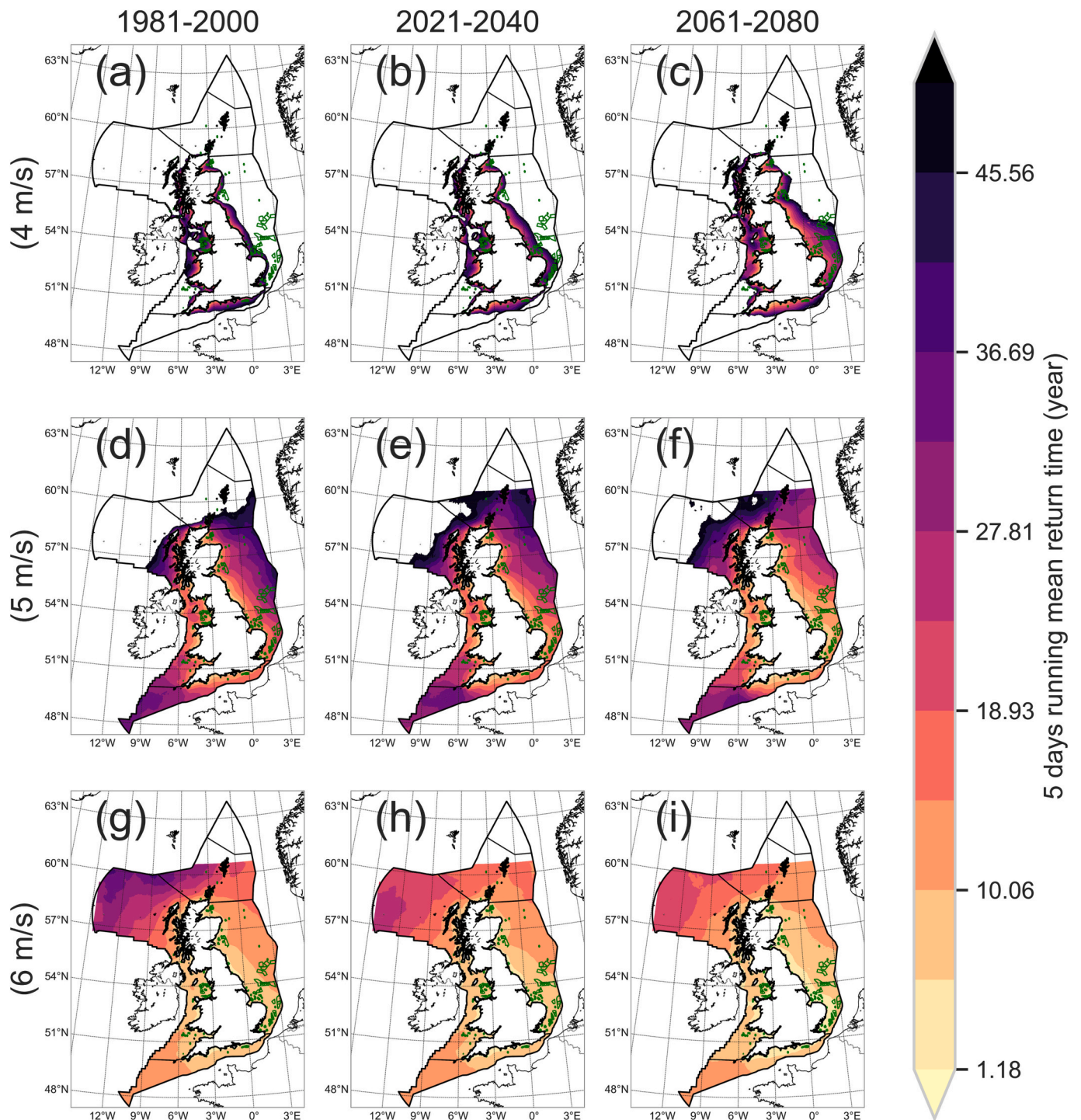


Fig. 11. Return time for three different thresholds for five days running mean in years. Columns from left to right represent the 1981–2000, 2021–2040, and 2061–2080 periods. Rows from top to bottom represent 4 m/s, 5 m/s, and 6 m/s. The green lines represent the UK Contract for different bidding rounds: Round 1, Round 2, Round 3, and Round 4, as well as the floating wind farms location. (Colour should be used in print). (For interpretation of the references to colour in this figure legend, the reader is referred to the web version of this article.)

emphasize the importance of combining wind with other renewable energy sources, such as solar and hydropower and having the ability to manage electricity demand effectively during times when wind speeds are low, particularly during the summer season. Alternatively, targeting seasons with less risk of future increase in low wind speed, such as the spring season, specifically in the West region, exhibits a decrease in durations occurring in the two future periods compared to the historical period.

Using five-day running mean data in return time analysis showed that the likelihood of experiencing LWE for wind speeds of 4 m/s, 5 m/s, and 6 m/s is higher near the shore in OWF locations than in open sea locations. In the three climate periods, most locations in the EEZ that utilize OWT with a cut-in wind speed of 6 m/s are at risk of frequent LWE with a return period of up to 20 years. Moreover, using a five-day running mean data, the North and West regions are the only regions with a negligible change in the return period regional median in two

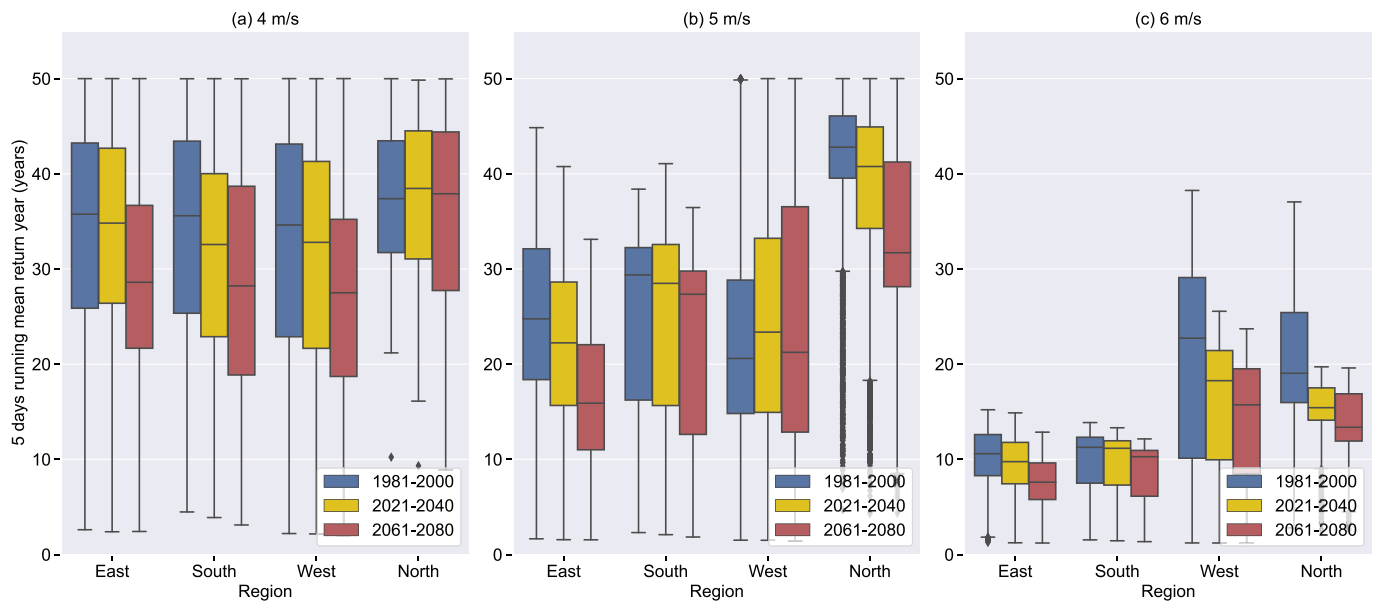


Fig. 12. Box plot of return year of (a) 4 m/s, (b) 5 m/s, and (c) 6 m/s using five days running mean for three periods (1981–2000 (blue), 2021–2040 (yellow), 2061–2080 (red)). Each plot's four comparison panels are the four regions, East, South, West, and North, respectively. The box holds the interquartile ranges (IQR), and the midline represents the median. The whiskers show the maximum and minimum values. The thin vertical black line represents the rest of the distribution, except for points determined to be "outliers". (Colour should be used in print). (For interpretation of the references to colour in this figure legend, the reader is referred to the web version of this article.)

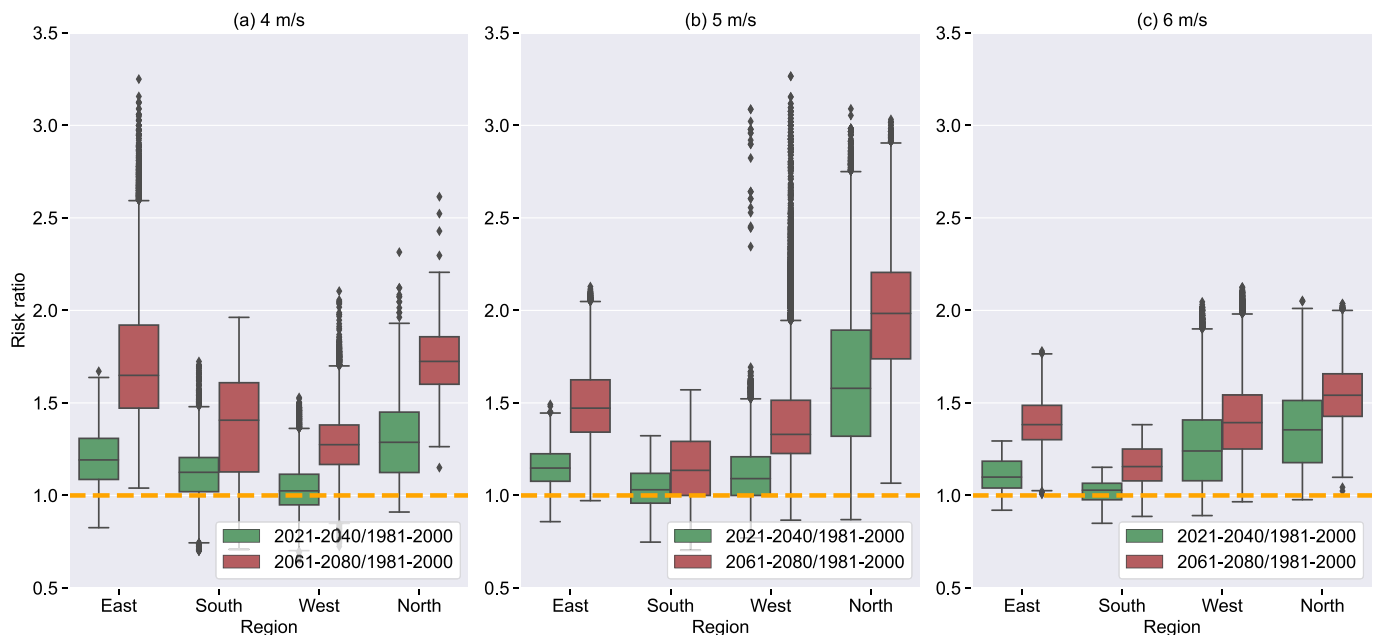


Fig. 13. Box plot of RR for 2021–2040 relative to 1981–2000 (green) and 2061–2080 relative to 1981–2000 (red) calculated for (a) 4 m/s, (b) 5 m/s, and (c) 6 m/s using five days running mean. Each plot's four comparison panels are the four regions, East, South, West, and North, respectively. The box holds the interquartile ranges (IQR), and the midline represents the median. The whiskers show the maximum and minimum values. The thin vertical black line represents the rest of the distribution, except for points determined to be "outliers". (Colour should be used in print). (For interpretation of the references to colour in this figure legend, the reader is referred to the web version of this article.)

future periods.

compared to the baseline period for the 4 m/s and 5 m/s thresholds, respectively. In an attempt to assess more extreme conditions for LWE, the North region remains recommended 4 m/s in 6- and 7-days running mean in the 2021–2040 period compared to the historical period, and the West region has the lowest risk for more frequent 4 m/s in 6-, 7, and 8-days for the.

near future period compared to the historical period. To reduce

exposure to the intense magnitude of LWE, it is suggested to develop WT's that can produce power at wind speeds below 3 m/s in locations near the coastline or install storage units or alternative generation sources to meet demand in case of using higher value thresholds in these locations. Also, future planning is needed to target the installation of future OWF models with a specific cut-in wind speed in regions with less risk for more frequent future low wind speed, such as the North region in case of using 4 m/s threshold and West region when using 5 m/s wind

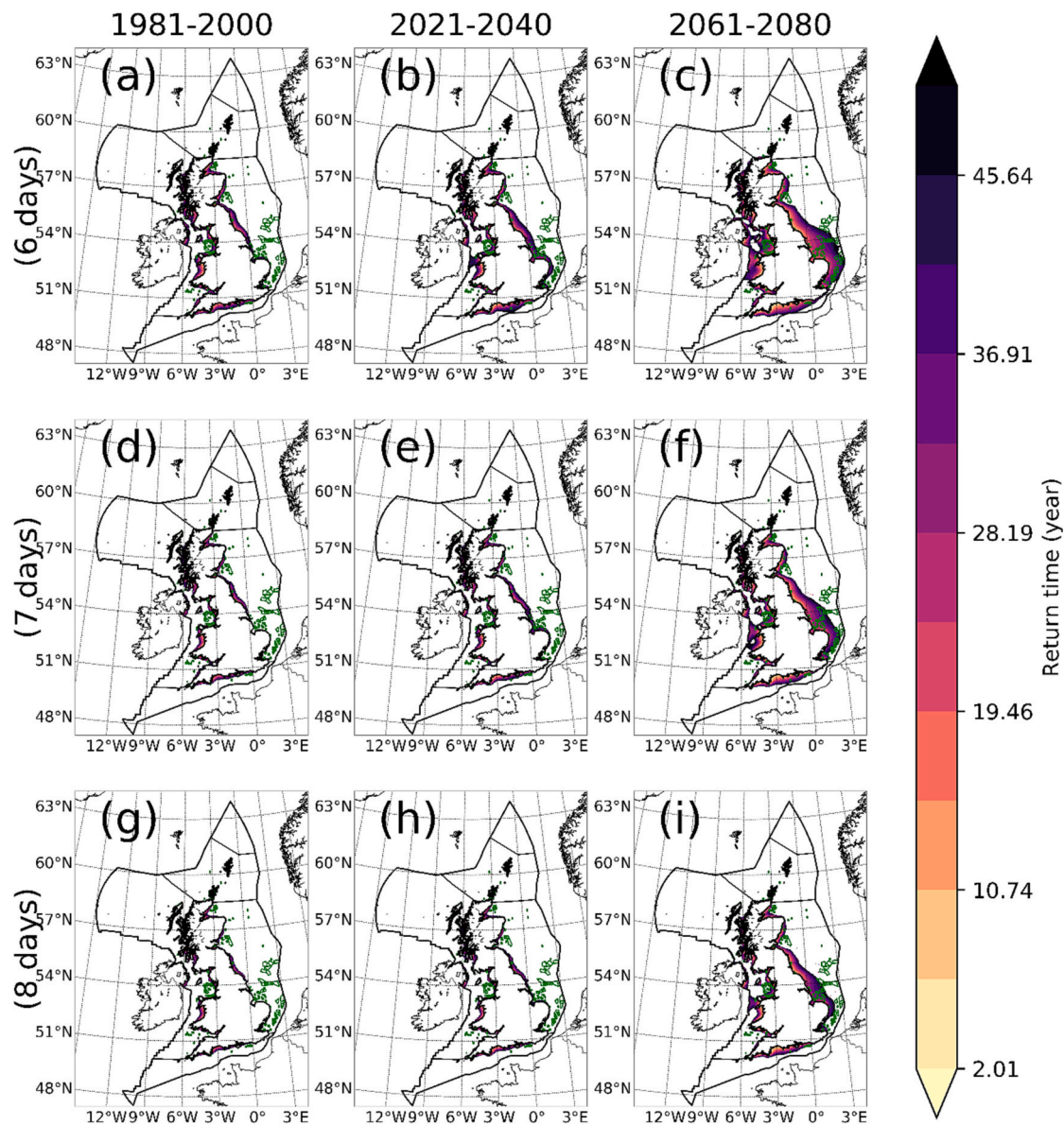


Fig. 14. Return time for 4 m/s in years using 6-, 7-, and 8-days running mean. Columns from left to right represent the 1981–2000, 2021–2040, and 2061–2080 periods. Rows from top to bottom represent a running mean of 6-, 7-, and 8-days. The green lines represent the UK Contract for different bidding rounds: Round 1, Round 2, Round 3, and Round 4, as well as the floating wind farms location. (Colour should be used in print). (For interpretation of the references to colour in this figure legend, the reader is referred to the web version of this article.)

turbine cut-in wind speed.

As a future work for the study approach, assessing the severity of storm surges and extreme wave height could provide valuable insights for future OWF siting. Utilizing diverse energy resource data, including wind and wave datasets, can enhance the overall decision-making process for the siting of hybrid renewable energy systems. Such an approach would lead to a more integrated and effective strategy for developing renewable energy resources.

6. Conclusion remarks

Motivated by the UK government's efforts for a more sustainable energy model to meet its net-zero target, this study delves into the topic of LWE and its impact on WT energy production. Using the UKCP18 daily mean wind speed at 151 m hub height, we aim to provide a comprehensive understanding of the characteristics and risks of LWE in the future through four analysis that covers various risks of low wind speed, such as change in the mean of the distribution, future change in

the left tail of the distribution under specific low wind speed percentile, the LWE persistence occurring, and the future change in return time occurrence of low wind speed event. Currently approximately 61% of wind farms are installed in the east coast of the UK. To recommend locations resilient to future LWE, the research compares four regions (East, South, West, and North); collectively, the regions cover the UK EEZ.

The main findings of this study can be summarized as follows:

- A seasonal investigation for the percentile corresponding to the most common range of low wind speed found that the 8th percentile was the best to cover the most common range of cut-in wind speed (3 m/s to 6 m/s) across seasons, as a result for the future change calculation for the 8th percentile of wind speed, the future planning for future OWF installation must consider alternative energy production source in summer season to meet the demand in East, West, and North EEZ regions.
- The duration of low wind speed was investigated in a seasonal period, confirming the risk of persistent low wind speed occurring in

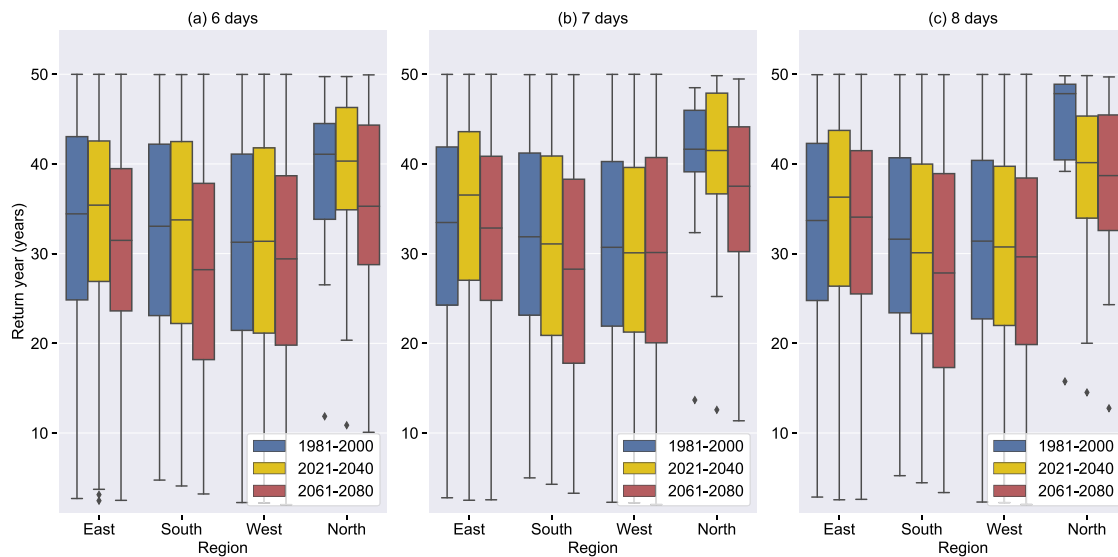


Fig. 15. Box plot of return year of 4 m/s using (a) 6 days, (b) 7 days, and (c) 8 days (running mean) using three periods (1981–2000 (blue), 2021–2040 (yellow), 2061–2080 (red)). Each plot's four comparison panels are the four regions, East, South, West, and North, respectively. The box holds the interquartile ranges (IQR), and the midline represents the median. The whiskers show the maximum and minimum values. The thin vertical black line represents the rest of the distribution, except for points determined to be “outliers”. (Colour should be used in print). (For interpretation of the references to colour in this figure legend, the reader is referred to the web version of this article.)

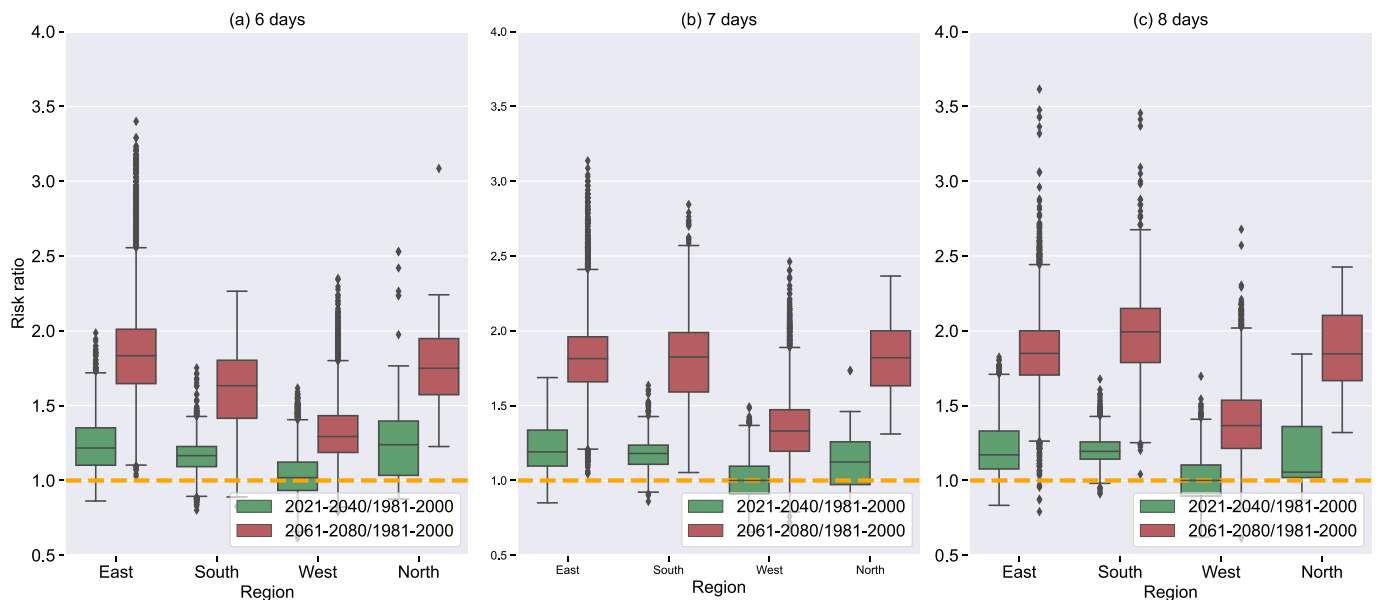


Fig. 16. Box plot of RR exceeding 4 m/s for 2021–2040 relative to 1981–2000 (green) and 2061–2080 relative to 1981–2000 (red) calculated for (a) 6 days, (b) 7 days, and (c) 8 days (running mean). Each plot's four comparison panels are the four regions, East, South, West, and North, respectively. The horizontal orange line point toward value =1, representing no change threshold. The box holds the interquartile ranges (IQR), and the midline represents the median. The whiskers show the maximum and minimum values. The thin vertical black line represents the rest of the distribution, except for points determined to be “outliers”. (Colour should be used in print). (For interpretation of the references to colour in this figure legend, the reader is referred to the web version of this article.)

the 2061–2080 period in summer seasons, where far future periods show an increase occurring compared to the historical period in most duration across all regions.

- The return time calculations for the 4 m/s threshold for the historical and two future periods using the Beta distribution, which was found to fit best the 5-, 6-, 7-, and 8-days running mean dataset, resulted in emphasizing the importance of consider future planning of wind turbines with cut-in wind speed <4 m/s in locations near to the coastline. Moreover, the research finding found a similarity between the future change in the statistic region median for the calculated return year and the corresponding RR calculations, leading to

recommend the South as a region with a lower risk of the more frequent occurrence of cut-in wind speed threshold in the 2021–2040 period compared to historical period using 5 m/s and 6 m/s cut-in wind speed thresholds and recommend the West region for 4 m/s investigation in 6-, 7-, and 8-days in the same future time period.

Certain regions within the UK EEZ are susceptible to an increased risk of more severe extreme LWE, while other regions may experience reduced risks. Consequently, when installing future OWTs, a careful assessment and evaluation of suitable locations are imperative. Factors such as the anticipated intensity of LWE events should be carefully

considered to ensure the optimal siting of these turbines.

CRedit authorship contribution statement

Sara Abdelaziz: Writing – review & editing, Writing – original draft, Visualization, Validation, Software, Methodology, Investigation, Funding acquisition, Formal analysis, Data curation. **Sarah N. Sparrow:** Writing – review & editing, Supervision, Methodology, Conceptualization. **WeiQi Hua:** Writing – review & editing. **David C.H. Wallom:** Writing – review & editing, Supervision, Conceptualization.

Declaration of Competing Interest

The authors declare the following financial interests/personal relationships which may be considered as potential competing interests:

The co-author WeiQi Hua work as Young Editorial Board Members in applied energy Journal.

Data availability

The UKCP18 dataset is available online at <https://catalogue.ceda.ac.uk/uuid/9842e395f2d04f48a177c3550756bf98>.

Acknowledgment

Funding: The Schlumberger Foundation Faculty for the Future program partially supported this research work.

The authors would like to acknowledge the use of the University of Oxford Advanced Research Computing (ARC) <https://doi.org/10.5281/zenodo.22558>.

Appendix A. Supplementary data

Supplementary data to this article can be found online at <https://doi.org/10.1016/j.apenergy.2023.122218>.

References

- [1] Edenhofer O. Accidents and risks BT - IPCC Special Report on Renewable Energy Sources and Climate Change Mitigation. 2011 [Online]. Available: [papers2://publication/uuid/7656EAF4-9B72-48D8-B960-300B0C7A388A](https://publications/uuid/7656EAF4-9B72-48D8-B960-300B0C7A388A).
- [2] Henderson AR, Morgan C, Smith B, Sørensen HC, Barthelmie RJ, Boesmans B. Offshore wind energy in Europe - a review of the state-of-the-art. *Wind Energy* 2003;6(1):35–52. <https://doi.org/10.1002/we.82>.
- [3] Bento N, Fontes M. Emergence of floating offshore wind energy: technology and industry. *Renew Sustain Energy Rev* 2019;99(October 2018):66–82. <https://doi.org/10.1016/j.rser.2018.09.035>.
- [4] Stefanakou AA, Nikitakos N, Lilas T, Pavlogeorgatos G. A GIS-based decision support model for offshore floating wind turbine installation. *Int J Sustain Energy* 2019;38(7):673–91. <https://doi.org/10.1080/14786451.2019.1579814>.
- [5] Carreno-Madinabeitia S, Ibarra-Berastegi G, Sáenz J, Ulazia A. Long-term changes in offshore wind power density and wind turbine capacity factor in the Iberian Peninsula (1900–2010). *Energy* 2021;226. <https://doi.org/10.1016/j.energy.2021.120364>.
- [6] Solbrekke IM, Sorteberg A. NORA3-WP: a high-resolution offshore wind power dataset for the Baltic, north, Norwegian, and Barents seas. *Sci Data* 2022;9(1):1–12. <https://doi.org/10.1038/s41597-022-01451-x>.
- [7] Hdidouan D, Staffell I. The impact of climate change on the levelised cost of wind energy. *Renew Energy* 2017;101:575–92. <https://doi.org/10.1016/j.renene.2016.09.003>.
- [8] Elsner P. Continental-scale assessment of the African offshore wind energy potential: Spatial analysis of an under-appreciated renewable energy resource. *Renew. Sustain. Energy Rev* 2019;104(July 2018):394–407. <https://doi.org/10.1016/j.rser.2019.01.034>.
- [9] Rusu E. Assessment of the wind power dynamics in the North Sea under climate change conditions. *Renew Energy* 2022;195:466–75. <https://doi.org/10.1016/j.renene.2022.06.048>.
- [10] Cai Y, Bréon FM. Wind power potential and intermittency issues in the context of climate change. *Energy Convers Manage* 2021;240. <https://doi.org/10.1016/j.enconman.2021.114276>.
- [11] Costoya X, deCastro M, Carvalho D, Feng Z, Gómez-Gesteira M. Climate change impacts on the future offshore wind energy resource in China. *Renew Energy* 2021;175:731–47. <https://doi.org/10.1016/j.renene.2021.05.001>.
- [12] SSE. Notification of closed period. <https://www.sse.com/news-and-views/2021/09/notification-of-close-period/>; 2023 (accessed Dec. 18, 2022).
- [13] IPCC. Foreword technical and preface. 2019.
- [14] IPCC. Climate change 2021 the physical science basis WGI. 2021.
- [15] Ranasinghe. Chapter 12: Climate change information for regional impact and for risk assessment. In: *Clim. Chang. 2021 Phys. Sci. Basis. Contrib. Work. Gr. I to Sixth Assess. Rep. Intergov. Panel Clim. Chang.* August 2021; 2021. p. 351–64.
- [16] Cavazzi S, Dutton AG. An offshore wind energy geographic information system (OWE-GIS) for assessment of the UK's offshore wind energy potential. *Renew Energy* 2016;87(2016):212–28. <https://doi.org/10.1016/j.renene.2015.09.021>.
- [17] Bahaj ABS, Mahdy M, Alghamdi AS, Richards DJ. New approach to determine the importance index for developing offshore wind energy potential sites: supported by UK and Arabian peninsula case studies. *Renew Energy* 2020;152:441–57. <https://doi.org/10.1016/j.renene.2019.12.070>.
- [18] Tegou L, Polatidis H, Haralambopoulos DA. Environmental management framework for wind farm siting: methodology and case study. *J Environ Manage* 2010;91(11):2134–47. <https://doi.org/10.1016/j.jenvman.2010.05.010>.
- [19] Díaz H, Soares CG. A multi-criteria approach to evaluate floating offshore wind farms siting in the Canary Islands (Spain). *Energies* 2021;14(4):865. <https://doi.org/10.3390/en14040865>.
- [20] Díaz H, Soares CG. An integrated GIS approach for site selection of floating offshore wind farms in the Atlantic continental European coastline. *Renew Sustain Energy Rev* 2020;134(September):110328. <https://doi.org/10.1016/j.rser.2020.110328>.
- [21] Vinhoza A, Schaeffer R. Brazil's offshore wind energy potential assessment based on a spatial multi-criteria decision analysis. *Renew Sustain Energy Rev* 2021;146 (May):111185. <https://doi.org/10.1016/j.rser.2021.111185>.
- [22] Juan D, Villacreses G, Gaona G, Martínez-g J. Wind farms suitability location using geographical information system (GIS), based on multi-criteria decision making (MCDM) methods: the case of continental Ecuador. *Renew Energy, Elsevier* 2017;109:275–86. <https://doi.org/10.1016/j.renene.2017.03.041>.
- [23] Schillings C, Wanderer T, Cameron L, van der Wal JT, Jacquemin J, Veum K. A decision support system for assessing offshore wind energy potential in the North Sea. *Energy Policy* 2012;49:541–51. <https://doi.org/10.1016/j.enpol.2012.06.056>.
- [24] Cradden L, Kalogeri C, Barrios IM, Galanis G, Ingram D, Kallos G. Multi-criteria site selection for offshore renewable energy platforms. *Renew Energy* 2016;87:791–806. <https://doi.org/10.1016/j.renene.2015.10.035>.
- [25] Pryor SC, Barthelmie RJ. A global assessment of extreme wind speeds for wind energy applications. *Nat Energy* 2021;6(3):268–76. <https://doi.org/10.1038/s41560-020-00773-7>.
- [26] Mytilinou V, Lozano-Minguez E, Kolios A. A framework for the selection of optimum offshore wind farm locations for deployment. *Energies* 2018;11(7). <https://doi.org/10.3390/en11071855>.
- [27] Zheng C, Wei, Li C, Yin, Xu J. Micro-scale classification of offshore wind energy resource: a case study of the New Zealand. *J Clean Prod* 2019;226:133–41. <https://doi.org/10.1016/j.jclepro.2019.04.082>.
- [28] Ohlendorf N, Schill WP. Frequency and duration of low-wind-power events in Germany. *Environ Res Lett* 2020;15(8). <https://doi.org/10.1088/1748-9326/ab91e9>.
- [29] Cannon DJ, Brayshaw DJ, Methven J, Coker PJ, Lenaghan D. Using reanalysis data to quantify extreme wind power generation statistics: a 33 year case study in Great Britain. *Renew Energy* 2015;75:767–78. <https://doi.org/10.1016/j.renene.2014.10.024>.
- [30] van der Wiel K, Stoop LP, van Zuijlen BRH, Blackport R, van den Broek MA, Selten FM. Meteorological conditions leading to extreme low variable renewable energy production and extreme high energy shortfall. *Renew Sustain Energy Rev* 2019;111(March):261–75. <https://doi.org/10.1016/j.rser.2019.04.065>.
- [31] Dawkins L, Rushby I. Characterising Adverse Weather for the UK Electricity System, including addendum for surplus generation events [Online]. Available: www.metoffice.gov.uk; 2020.
- [32] Patlakas P, Galanis G, Diamantis D, Kallos G. Low wind speed events: persistence and frequency. *Wind Energy* 2017;(January):1–20. <https://doi.org/10.1002/we.2078>.
- [33] Leahy PG, McKeogh EJ. Persistence of low wind speed conditions and implications for wind power variability. *Wind Energy* 2012;(May 2012):1–20. <https://doi.org/10.1002/we.1509>.
- [34] Khaliq MN, St-Hilaire A, Ouarda TBMJ, Bobée B. Frequency analysis and temporal pattern of occurrences of southern Quebec heatwaves. *Int J Climatol* 2005;25(4):485–504. <https://doi.org/10.1002/joc.1141>.
- [35] Weber J, et al. Wind power persistence characterized by Superstatistics. *Sci Rep* 2019;9(1):1–15. <https://doi.org/10.1038/s41598-019-56286-1>.
- [36] Konneh D, Howlader H, Shigenobu R, Senjyu T, Chakraborty S, Krishna N. A multi-criteria decision maker for grid-connected hybrid renewable energy systems selection using multi-objective particle swarm optimization. 2019. <https://doi.org/10.3390/su11041188>.
- [37] CEDA. UK Climate Projections 2018 (UKCP18). <https://catalogue.ceda.ac.uk/uuid/c700e47ca54d4c43b213fe879863d589?ga=2.164002815.1334446900.1624300753-1212288270.1616941503>; 2023 (accessed Jun. 22, 2021).
- [38] Kendon EJ, et al. UKCP convection-permitting model projections: Science report. 2019.
- [39] Met Office. UKCP18 Factsheet: UKCP Local (2.2km) Projections [Online]. Available: www.metoffice.gov.uk; 2019.
- [40] Cotterill D, Stott P, Christidis N, Kendon E. Increase in the frequency of extreme daily precipitation in the United Kingdom in autumn. *Weather Clim Extrem* 2021;33:100340. <https://doi.org/10.1016/j.wace.2021.100340>.

- [41] Wang H. Quantitative modelling of climate change impact on hydro-climatic extremes. 2021.
- [42] Hersbach H, et al. Global reanalysis: goodbye ERA-interim, Hello ERA5. 2019. <https://doi.org/10.21957/vf291hehd7>.
- [43] Olauson J. ERA5: the new champion of wind power modelling? *Renew Energy* 2018;126:322–31. <https://doi.org/10.1016/j.renene.2018.03.056>.
- [44] Pryor SC, Barthelmie RJ. A global assessment of extreme wind speeds for wind energy applications. *Nat Energy* 2021;6(3):268–76. <https://doi.org/10.1038/s41560-020-00773-7>.
- [45] Hayes L, Stocks M, Blakers A. Accurate long-term power generation model for offshore wind farms in Europe using ERA5 reanalysis. *Energy* 2021;229:120603. <https://doi.org/10.1016/j.energy.2021.120603>.
- [46] Costoya X, deCastro M, Santos F, Sousa MC, Gómez-Gesteira M. Projections of wind energy resources in the Caribbean for the 21st century. *Energy* 2019;178:356–67. <https://doi.org/10.1016/j.energy.2019.04.121>.
- [47] Costoya X, deCastro M, Carvalho D, Gómez-Gesteira M. On the suitability of offshore wind energy resource in the United States of America for the 21st century. *Appl Energy* 2020;262(January):114537. <https://doi.org/10.1016/j.apenergy.2020.114537>.
- [48] Perkins SE, Pitman AJ, Holbrook NJ, McAneney J. Evaluation of the AR4 climate models' simulated daily maximum temperature, minimum temperature, and precipitation over Australia using probability density functions. *J Climate* 2007;20(17):4356–76. <https://doi.org/10.1175/JCLI4253.1>.
- [49] Santos F, et al. On the accuracy of CORDEX RCMs to project future winds over the Iberian Peninsula and surrounding ocean. *Appl Energy* 2018;228(May):289–300. <https://doi.org/10.1016/j.apenergy.2018.06.086>.
- [50] Wiser R, et al. Expert elicitation survey predicts 37% to 49% declines in wind energy costs by 2050. *Nat Energy* 2020;14. <https://doi.org/10.1038/s41560-021-00810-z>.
- [51] Krut B, Lehning M, Kahl A. Potential contributions of wind power to a stable and highly renewable Swiss power supply. *Appl Energy* 2017;192:1–11. <https://doi.org/10.1016/j.apenergy.2017.01.085>.
- [52] Grassi S, et al. Mapping of the global wind energy potential using open source GIS data. In: 2nd Int. Conf Energy Environ bringing together Eng Econ, no. June; 2015. p. 6 [Online]. Available, https://www.renewables-now.ch/20150618_Grassi_Prepr_int_ICEE2015.pdf.
- [53] MMO. United Kingdom commercial sea fisheries landings by Exclusive Economic Zone of Capture [Online]. Available, https://www.gov.uk/government/uploads/system/uploads/attachment_data/file/647579/United_Kingdom_commercial_sea_fisheries_landings_by_Exclusive_Economic_Zone_of_capture_2012_2016.pdf; 2017.
- [54] Library NM. Fact sheet 8 — The Shipping Forecast National Meteorological Library and Archive. 2023.
- [55] Dawkins LC. Weather and climate change risks in a highly renewable UK energy system: literature review [Online]. Available: <https://www.preventionweb.net/publications/view/66394>; 2019.
- [56] Dueñas-Osorio L, Basu B. Unavailability of wind turbines due to wind-induced accelerations. *Eng Struct* 2008;30(4):885–93. <https://doi.org/10.1016/j.engstruct.2007.05.015>.
- [57] Hanif MA, Nadeem F, Tariq R, Rashid U. Wind Energy and its Harnessing Systemsno. 1; 2022.
- [58] Ho L, Fiedler S. Climatology of low wind and solar power production events in Europe with Grosswetterlagen classificationno. 2; 2022. p. 10164.
- [59] Kavianpour M, Seyedabadi M, Moazami S, Yamini OA. Copula based spatial analysis of drought return period in southwest of Iran. *Period Polytech Civ Eng* 2020;64(4):1051–63. <https://doi.org/10.3311/PPci.16301>.
- [60] Afshar MH, Şorman AÜ, Tosunoğlu F, Bulut B, Yılmaz MT, Danandeh Mehr A. Climate change impact assessment on mild and extreme drought events using copulas over Ankara, Turkey. *Theor Appl Climatol* 2020;141(3–4):1045–55. <https://doi.org/10.1007/s00704-020-03257-6>.
- [61] Hogesteegeer S, Singh R, Holden P, Fu NS, Odoulami RC. Anthropogenic influence on the drivers of the Western Cape drought 2015–2017. *Environ Res Lett* 2018;13. <https://doi.org/10.1088/1748-9326/aae9f9>.
- [62] Croxton FE, Cowden DJ. The frequency distribution. *Appl Gen Stat* 2011;164–93. <https://doi.org/10.1037/13608-008>.
- [63] Barrios R, Dios F. Exponentiated Weibull distribution family under aperture averaging for Gaussian beam waves. 2012.
- [64] Nedaei M, Assareh E, Walsh PR. A comprehensive evaluation of the wind resource characteristics to investigate the short term penetration of regional wind power based on different probability statistical methods. *Renew Energy* 2020;128(2018): 362–74. <https://doi.org/10.1016/j.renene.2018.05.077>.
- [65] Saleh ME. An introduction to probability and statistics. Second. WILEY; 2000.
- [66] Otto FEL, Philip S, Kew S, Li S, King A, Cullen H. Attributing high-impact extreme events across timescales—a case study of four different types of events. *Clim Change* 2018;149(3–4):399–412. <https://doi.org/10.1007/s10584-018-2258-3>.
- [67] Bellprat O, Guemas V, Doblas-Reyes F, Donat MG. Towards reliable extreme weather and climate event attribution. *Nat Commun* 2019;10(1):29–31. <https://doi.org/10.1038/s41467-019-09729-2>.